HHS Public Access

Author manuscript

Sci Immunol. Author manuscript; available in PMC 2024 January 23.

Published in final edited form as:

Sci Immunol. 2023 August 04; 8(86): eadg0878. doi:10.1126/sciimmunol.adg0878.

Sustained CD28 costimulation is required for self-renewal and differentiation of TCF-1^{+} PD-1^{+} CD8 T cells

Etienne Humblin[1], **Isabel Korpas**[1], **Jiahua Lu**[1], **Dan Filipescu**[2], **Verena van der Heide**[1], **Simon Goldstein**[1], **Abishek Vaidya**[1], **Alessandra Soares-Schanoski**[1,†], **Beatrice Casati**[1,‡], **Myvizhi E. Selvan**[3], **Zeynep H. Gümüş**[1,3], **Andreas Wieland**[4], **Mauro Corrado**[5], **Leona Cohen-Gould**[6], **Emily Bernstein**[2,7], **Dirk Homann**[1,8], **Jerry Chipuk**[2,7], **Alice O. Kamphorst**[1,2,7,*]

[1]Marc and Jennifer Lipschultz Precision Immunology Institute, Icahn School of Medicine at Mount sinai - ISMMS; New York, NY 10029, USA

[2]Department of Oncological Sciences, ISMMS; New York, NY 10029, USA

[3]Department of Genetics and Genomics, ISMMS; New York, NY 10029, USA

[4]Department of Otolaryngology-Head and Neck Surgery and Pelotonia Institute for Immuno-Oncology, OSUCCC – James, The Ohio State University, Columbus, OH 43210, USA.

[5]Cologne Excellence Cluster on Cellular Stress Responses in Aging-Associated Diseases (CECAD); Center for Molecular Medicine (CMMC) and Institute for Genetics, University of Cologne, 50931 Cologne, Germany

[6]Department of Biochemistry, Weill Cornell Medical College; New York, NY 10029, USA;

[7]Tisch Cancer Institute, ISMMS; New York, NY 10029, USA

[8]Diabetes Obesity Metabolism Institute, ISMMS; New York, NY 10029, USA

Abstract

During persistent antigen stimulation, such as in chronic infections and cancer, CD8 T cells differentiate into a hypofunctional PD-1^{+} exhausted state. Exhausted CD8 T cell responses are maintained by precursors (Tpex) that express the transcription factor T cell factor (TCF)-1 and high levels of the costimulatory molecule CD28. Here, we demonstrate that sustained CD28 costimulation is required for maintenance of anti-viral T cells during chronic infection. Low-level CD28 engagement preserved mitochondrial fitness and self-renewal of Tpex, whereas stronger CD28 signaling enhanced glycolysis and promoted Tpex differentiation into TCF-1^{neg} exhausted

*Corresponding author. alice.kamphorst@mssm.edu.

†Present address: RVAC Medicines, Waltham, MA 02451, USA

‡Present address: Division of Immune Diversity, Department of Immunology and Cancer, German Cancer Research Centre (DKFZ) and Faculty of Biosciences, Heidelberg University 69120 Heidelberg, Germany

Author contributions:

EH and AOK conceived the study. EH, DF and AOK developed the methodology. EH, IK, JL, DF, VH, SG, AV, ASS, BC, LCG, MC, AW and AOK performed experiments. EH and AOK analyzed the data. DF and MES performed RNA sequencing anaylsis. EH and AOK drafted the manuscript. ZHG, EB, DH and JC provided critical expertise and experimental ideas. AOK obtained funding and supervised the study. All authors were involved in the critical review of the manuscript. All authors read and approved the manuscript.

Competing interests:

The other authors declare that they have no competing interests.

CD8 T cells (Tex). Importantly, enhanced differentiation by CD28 engagement did not reduce the Tpex pool. Together these findings demonstrate that continuous CD28 engagement is needed to sustain PD-1^{+} CD8 T cells and suggest that increasing CD28-signaling promotes Tpex differentiation into more functional effector-like Tex, possibly without compromising long-term responses.

One-Sentence Summary:

CD28 modulates the metabolism of PD-1^{+} CD8 T cells and is required to sustain responses during chronic antigen stimulation.

INTRODUCTION

T cells persistently exposed to antigen acquire a distinct gene expression program which imparts attenuated effector function, reduced proliferative capacity, compromised metabolic fitness and high expression of inhibitory receptors, such as Programmed Cell Death-1 (PD-1) (1, 2). CD8 T cell responses during chronic stimulation are sustained by T Cell Factor-1 (TCF-1)$^{+}$ PD-1^{+} CD8 T cells that function as stem-like progenitor cells (Tpex) to exhausted TCF-1^{neg} PD-1^{+} CD8 T cells (Tex) (1, 3–6). First described in murine chronic infection with lymphocytic choriomeningitis virus (LCMV) (4, 6), Tpex have also been identified in tumor models (7, 8), cancer patients (7, 9–12), as well as in type I diabetes (13, 14). TCF-1^{+} PD-1^{+} Tpex self-renew to preserve persistent T cell responses and are also responsible for the proliferative burst that generates effector-like cells following PD-1 blockade therapy (4, 6–8). In cancer patients, Tpex differentiation has been proposed to sustain tumor CD8 T cell infiltration (9), and intratumoral TCF-1^{+} CD8 T cells were predictive of response to immunotherapy (10).

In mice chronically infected with LCMV, Tpex predominantly reside in the T-cell zone of lymphoid organs and do not re-circulate (15). In tumor lesions, TCF-1^{+} CD8 T cells are found in antigen-presenting cell (APC)-rich niches (9, 12). In liver cancer patients, we recently reported that intratumoral dendritic cell-helper CD4 T cell niches may promote effective differentiation of Tpex following PD-1 blockade therapy (12). In accordance with those findings, Prokhnevska et al demonstrated that Tpex differentiate and acquire an effector program based on signals received at tumor sites (16). These observations underlie the requirement of specific microenvironmental cues to promote Tpex survival and differentiation, and thus regulate longevity and efficacy of T cell responses. However, the determinants of self-renewal and differentiation of Tpex are still not well defined, and whether differentiation diminishes the Tpex pool and long-term T cell responses has not been addressed.

We previously showed that expansion of PD-1^{+} CD8 T cells following PD-1-targeted therapy is CD28-dependent (17). Tpex express high levels of CD28 (6) and localize in close proximity to APCs that express B7 proteins (CD28 ligands, CD80 and CD86) (9, 12, 18). Here, we sought to address the effects of CD28 engagement on Tpex self-renewal and differentiation. We demonstrate that the CD28/B7 pathway is necessary to maintain virus-specific CD8 T cells during chronic LCMV infection. Whereas low CD28 signaling was

required for Tpex self-renewal, stronger levels of CD28 costimulation were necessary for differentiation into Tex. Mechanistically, we uncovered that low sustained CD28 signaling during persistent antigen stimulation is essential to maintain mitochondrial fitness. However, stronger CD28 signaling on Tpex was associated with increased glycolysis, higher levels of the transcription factor interferon regulatory factor 4 (IRF4) and differentiation into more effector-like Tex. Last, we show that improving Tpex differentiation by enhancing CD28 signaling does not impair Tpex self-renewal, suggesting that CD28 costimulation can promote more effective and long-lasting PD-1^+ CD8 T cell responses.

RESULTS

Sustained B7-costimulation is required for the maintenance of virus-specific CD8 T cells in established chronic LCMV infection

To determine the impact of the CD28/B7 pathway on the dynamics of PD-1^+ CD8 T cells, we utilized the mouse model of life-long chronic LCMV infection in which CD4 T cells are transiently depleted during priming, resulting in constant antigen load (19). Using this model, we previously reported that transient blockade of B7 ligands did not affect the number of virus-specific CD8 T cells (Fig. S1) and (17). Tpex express high levels of CD28 compared to Tex (Fig. S2) and are responsible for maintaining PD-1^+ CD8 T cell responses during chronic antigen stimulation by self-renewal and differentiation. As Tpex undergo slow self-renewal, we reasoned that longer treatment would be required to study the role of the CD28/B7 pathway on the dynamics of PD-1^+ CD8 T cells. Following 7 weeks of B7 blockade in mice with established life-long chronic LCMV infection (Fig. 1A), we observed a drastic decrease in frequency (Fig. 1B and 1C) and absolute numbers (Fig. 1D) of virus-specific CD8 T cells in the spleen. Likewise, LCMV-specific CD8 T cells in the liver and lung were also markedly reduced by 7 weeks of B7 blockade (Fig. 1E). We also observed a decrease in proliferation of virus-specific CD8 T cells as evaluated by Ki-67 staining (Fig. 1F and 1G), suggesting that sustained CD28 costimulation maintains proliferation of PD-1^+ CD8 T cells. Finally, in accordance with residual effector function of exhausted CD8 T cells, the decrease in virus-specific CD8 T cells resulted in increased viral load in spleen, liver and serum of B7 blockade-treated mice (Fig. 1H and S3A). These data show that during chronic viral infection the CD28/B7 pathway is required for long-term maintenance of virus-specific PD-1^+ CD8 T cells.

Despite the substantial effects of B7 blockade on the number of LCMV-specific CD8 T cells, the functionality of the remaining LCMV-specific CD8 T cells was not affected, as measured by frequency of IFN-γ or XCL-1 producing cells (Fig. S3B). Following 7 weeks of B7 blockade, there was a decrease in the absolute number of both Tpex (TCF-1^+ TIM-3^{neg}) and Tex (TCF-1^{neg} TIM-3^+) virus-specific CD8 T cells (Fig. 1I). However, B7 blockade did not affect the relative composition of virus-specific cells with regards to the major subsets of PD-1^+ CD8 T cells: within LCMV-specific CD8 T cells, there were no differences in the frequency of Tpex and Tex (TCF-1^{neg}) (Fig. 1J), not even when we assessed more functional “transitional” *effector-like* CX3CR1^+ cells (20, 21) (Fig. S3C). These data suggest that both Tpex self-renewal and differentiation are affected by blockade of the CD28/B7 pathway.

CD28 expression levels modulate the dynamics of PD-1$^+$ CD8 T cell subsets

Because B7 blockade will also interfere with CTLA-4 interactions and may affect additional cell types beyond virus-specific CD8 T cells, to assess the cell-intrinsic role of CD28 signaling on PD-1$^+$ CD8 T cells, we used inducible genetic deletion of *Cd28* on transgenic P14 CD8 T cells (specific for LCMV-GP33). P14 T cells that have one *Cd28* allele knock-out expressed about half of CD28 protein compared to wild-type cells (Fig. S4A–B), thus providing a way to address the impact of CD28 levels in CD8 T cell biology. Control *Cd28*$^{fl/fl}$ CreERT2^{neg} P14 T cells were co-transferred in a 50:50 ratio with either homozygous *Cd28*$^{fl/fl}$ CreERT2$^+$ P14 or heterozygous *Cd28*$^{fl/wt}$ CreERT2$^+$ P14 T cells expressing different congenic markers (Fig. 2A). Recipient mice were transiently depleted of CD4 T cells and infected with LCMV clone 13 to induce life-long chronic LCMV infection. All P14 T cells showed equivalent expansion following chronic infection (Fig. 2B), and tamoxifen administration resulted in deletion of CD28 in homozygous *Cd28*$^{fl/fl}$ P14 T cells (Fig. S4A and C, in about 50% of cells) and reduction of CD28 expression in heterozygous *Cd28*$^{fl/wt}$ P14 T cells (Fig. S4D). 45 days after tamoxifen administration, homozygous *Cd28*$^{fl/fl}$ CreERT2$^+$ P14 Tpex were reduced in frequency compared to control Tpex, while heterozygous *Cd28*$^{fl/wt}$ CreERT2$^+$ P14 Tpex remained with similar frequency as control Tpex (Fig. 2C). These data suggest that Tpex maintenance requires CD28, but low levels of CD28 costimulation are sufficient to maintain self-renewal. In contrast, both *Cd28*$^{fl/fl}$ CreERT2$^+$ and *Cd28*$^{fl/wt}$ CreERT2$^+$ P14 Tex represented a lower frequency than control P14 Tex (Fig. 2D). These results suggest that even a decrease in CD28 signaling may hinder Tpex differentiation into Tex. Accordingly, we found that proliferation of P14 TCF-1^{neg} Tex was diminished by deletion or reduction of CD28 (Fig. 2E and F). Together these data suggest that differentiation of Tpex may require higher levels of CD28 costimulation than self-renewal.

To assess if Tpex that develop in the presence of CD4-help would also require sustained CD28 costimulation, we performed similar experiments in mice chronically infected with LCMV without transient CD4 depletion (Fig. S5A). In accordance with our previous findings, we observed reduced proliferation in homozygous *Cd28*$^{fl/fl}$ CreERT2$^+$ P14 that had lost CD28 expression (Fig. S5B), and a similar trend was also noted when we compared heterozygous *Cd28*$^{fl/wt}$ CreERT2$^+$ P14 T cells (reduced CD28 expression) to control P14 T cells (Fig. S5C). These data support that, even with CD4-help, Tpex rely on continuous CD28 costimulation for maintenance of PD-1$^+$ CD8 T cell responses.

Interestingly, despite substantial differences in cell expansion, loss of CD28 did not result in overt phenotypic differences with regards to markers commonly used to identify and characterize different subsets of PD-1$^+$ CD8 T cells (Fig. 2G and S6A). Beyond a decrease in proliferative capacity, there were no differences in apoptosis and with regards to cytokine production, loss of CD28 resulted in only a small reduction in IFN-γ production among Tpex and CX3CR1^{neg} terminally differentiated Tex CD28^{neg} P14 T cells (Fig. S6).

CD28 is required for Tpex self-renewal and differentiation into Tex

To directly address if CD28 levels would impact Tpex fate, we performed adoptive transfer experiments. CellTrace Violet (CTV)-labeled CD45.2 CD28^{hi}, CD28^{int} and CD28^{neg}

Tpex - sorted from tamoxifen-treated chronically infected control *Cd28*$^{fl/fl}$ CreERT2^{neg}, heterozygous *Cd28*$^{fl/wt}$ CreERT2^{+} or homozygous *Cd28*$^{fl/fl}$ CreERT2^{+} mice – were transferred into infection-matched CD45.1 recipients (Fig. 3A and S7A–B). Recipient mice were analyzed five weeks after transfer, and we confirmed that CD28 levels on donor CD45.2 cells were consistent with pre-transfer levels (Fig. S7B and C). Mice that received control Tpex had substantially more donor cells in spleen (Fig. 3B and C) and lung (Fig. 3B and D) compared to mice that received CD28^{int} or CD28^{neg} Tpex. Control Tpex differentiated into TCF-1^{neg} CD39^{+} Tex, whereas CD28^{int} Tpex presented reduced ability to differentiate, and CD28^{neg} Tpex failed to convert into Tex (Fig. 3E–G). To evaluate Tpex self-renewal capacity we analyzed donor CD45.2^{+} cells that retained TCF-1 expression after proliferation (CTV^{neg}). The frequency and number of TCF-1^{+} cells that had divided (self-renewal) was not different between control and CD28^{int} Tpex, whereas it was strongly impaired in CD28^{neg} Tpex compared to control (Fig. 3H–J). To further determine the impact of CD28 costimulation on Tpex self-renewal and differentiation, we analyzed whether the progeny of Tpex (CTV^{low}) were more likely to become CD39^{+} differentiated Tex than undergo self-renewal (remain TCF-1^{+}) (Fig. 3K). We found that decreased CD28 expression had a stronger impact on Tpex differentiation than on self-renewal, reflected by lower frequency of TCF-1^{neg} CD39^{+} differentiated Tex among CTV^{low} CD28^{int} cells when compared to the progeny of control CD28^{hi} Tpex. These data demonstrate the requirement for CD28 costimulation for Tpex self-renewal and differentiation and show a stronger dependence on higher CD28 costimulation for Tpex conversion into Tex.

To address if CD4-help would overcome the requirement for CD28 costimulation for Tpex maintenance and differentiation, Tpex isolated from mice with life-long LCMV chronic infection (unhelped environment) were transferred into LCMV chronically infected recipients that had not been depleted of CD4 T cells (Fig. S8A). The fate of CD28^{hi}, CD28^{int} and CD28^{neg} Tpex was analyzed two weeks after transfer into a helped chronic infection environment. Consistent with lower viral load in helped chronic LCMV infection (19), all transferred cells, including control CD28^{hi}, displayed limited capacity to expand as shown by the low frequency and number of donor cells recovered in the spleen and lung of recipient animals (Fig. S8B, C and D). Accordingly, only a low frequency of control Tpex was able to convert into Tex (Fig. S8E, F and G) or to self-renew (Fig. S8H, I and J). Nevertheless, loss of CD28 virtually abrogated Tpex differentiation and self-renewal, whereas a decrease in CD28 expression diminished Tpex differentiation but did not impact self-renewal (Fig. S8E–K). These observations recapitulate our previous findings and show that sustained CD28 costimulation is critical for Tpex biology, even in the presence of CD4 T cell help.

CD28 is a central regulator of Tpex metabolism

In order to gain better insight into the molecular mechanisms by which CD28 costimulation modulates self-renewal and differentiation of PD-1^{+} CD8 T cells, we performed transcriptional analysis of control CD28^{hi} (control) and CD28^{neg} Tpex and Tex sorted from LCMV chronically infected mice (extended data file S1). Consistent with flow cytometry characterization, there were no major changes in the molecular programs characteristics of each subset upon CD28 deletion (Fig. S9A). In accordance with higher CD28 expression by Tpex (Fig. S2) these cells were more strongly affected by CD28 loss as shown by a

higher number of differentially regulated genes in Tpex than Tex (Fig. S9B). Gene set enrichment analyses (GSEA) revealed strong downregulation of oxidative phosphorylation (OXPHOS) in cells that lost CD28 expression (Fig. 4A, S9C and D, extended data file S2). Differential gene expression analysis confirmed downregulation of genes encoding several mitochondrial proteins (*Atp5e, Atp5d, Atp5c1, Atp5g3, Ndufc2, Ndufb6, Ndufa8, Ndufb5, Ndufs5, Ndufv1, Uqcrq, Uqcr11, Cox17, Sdhb*) or shown to regulate mitochondrial fitness (e.g. *Bhlhe40*) (22) (Fig. S9E).

Previous studies reported impaired metabolism with decreased mitochondrial fitness, loss of oxidative phosphorylation, and reduced glycolytic capacity of chronically stimulated PD-1^+ CD8 T cells (23–25). However, recent studies clarified that in contrast to terminally exhausted T cells, Tpex display higher mitochondrial fitness (26). To determine the effect of CD28 costimulation on Tpex oxidative phosphorylation, we performed metabolic flux analyses on sorted $CD28^{hi}$, $CD28^{int}$, and $CD28^{neg}$ Tpex isolated from mice with life-long LCMV infection. We analyzed mitochondrial respiration, using carbonyl cyanide-4 (trifluoromethoxy) phenylhydrazone (FCCP) to disrupt the mitochondrial membrane potential and observed that $CD28^{neg}$ Tpex presented a poor increase in oxygen consumption rate (OCR) compared to control and $CD28^{int}$ Tpex (Fig. 4B). Loss of CD28 profoundly affected Spare Respiratory Capacity (SRC), a measurement of mitochondrial capacity to meet energetic demands, whereas $CD28^{int}$ Tpex displayed comparable SRC to control (Fig. 4C). Mitochondrial dysfunction due to lack of CD28 signaling was also confirmed on Tpex isolated from chronically infected mice that received 7 weeks of B7-blockade (Fig. S10A and B). To further assess mitochondrial activity, we measured mitochondrial reactive oxygen species (ROS) production with MitoSOX staining. As previously reported (26), Tpex expressed high mitochondrial ROS, which was not affected in $CD28^{int}$ Tpex, but strongly decreased in $CD28^{neg}$ Tpex (Fig. 4D). Similar differences in mitochondrial ROS production were observed when we analyzed MitoSOX staining in P14 $CD28^{neg}$ Tpex generated during helped chronic LCMV infection (Fig. S11), emphasizing that sustained CD28 costimulation is also required to preserve Tpex metabolic fitness in the presence of CD4 helper T cells, and confirming that low levels of CD28 signaling are sufficient to promote oxidative phosphorylation. Finally, we assessed mitochondrial morphology using electron microscopy and found that control Tpex presented mitochondria with densely packed cristae that took up most of the volume of the matrix (Fig. 4E). In contrast, we observed that $CD28^{neg}$ Tpex had less distinct mitochondria with wider cristae associated with lower mitochondrial respiration efficiency (27, 28), whereas $CD28^{int}$ Tpex displayed a mixed phenotype (Fig. 4E and F). These data show that sustained CD28 signaling is required to maintain Tpex mitochondrial fitness.

Quiescent T cells, such as naïve or memory, rely mainly on OXPHOS to generate energy (29), while differentiation into an effector state requires a metabolic switch to glycolysis that is largely CD28-dependent (30–32). To assess the effect of CD28 signaling on Tpex glycolytic activity, we stimulated sorted $CD28^{hi}$, $CD28^{int}$ and $CD28^{neg}$ Tpex with αCD3 and αCD28 and measured extracellular acidification rate (ECAR) (Fig. 4G and H). Following αCD3/αCD28 stimulation, cells were treated with rotenone and antimycin (Rot/AA) to inhibit the mitochondrial electron transport chain and force glycolysis, to determine maximal glycolytic capacity and compensatory glycolysis. We observed a dose-

dependent effect of CD28 on Tpex glycolytic activity, glycolytic reserve and compensatory glycolysis (Fig. 4H). Although, 2-NBDG (a glucose analogue) uptake by T cells should be interpreted cautiously (33), we observed that even though this uptake was quite low at baseline, it increased after TCR-stimulation and was further enhanced in the presence of αCD28 agonist (Fig. 4I). Finally, because the transcription factor interferon regulatory factor 4 (IRF4) has been implicated in both glycolysis and Tpex/Tex dynamics (24, 34), we assessed whether CD28 signaling in Tpex would modulate IRF4 levels. Confirming our hypothesis, we observed that CD28 engagement increased expression levels of IRF4 induced by cognate peptide stimulation in Tpex (Fig. 4J). In sum, these data show that low CD28 signaling is sufficient to maintain mitochondrial fitness but stronger CD28 signaling increases glycolysis and nutrient uptake, potentially benefiting Tpex differentiation.

Enhancing CD28 signaling drives Tpex differentiation into effector-like Tex

To address if enhancing CD28 costimulation would improve Tpex differentiation and conversion into Tex, we cultured CTV-labeled Tpex isolated from chronically infected mice with αCD3 in the presence of high and low-dose agonistic αCD28. CD3 stimulation in absence of CD28 engagement failed to promote cell division leading neither to Tpex differentiation into TCF-1^{neg} Tex (Fig. S12A) nor self-renewal (Fig. S12B). αCD3 in combination with high-dose αCD28 induced both Tpex differentiation and self-renewal, whereas αCD3 combined with low-dose agonistic αCD28 promoted Tpex self-renewal (Fig. S12A and B). These ex vivo experiments confirm the importance of CD28 signaling for Tpex dynamics, and that Tpex self-renewal requires lower CD28 stimulation than differentiation.

To assess if we can improve the function of PD-1^{+} CD8 T cells by promoting CD28 signaling on Tpex, we sorted Tpex from LCMV chronically infected mice, with and without adding agonistic αCD28. Control CD28-untouched Tpex or Tpex bound by αCD28 agonistic antibodies were transferred into mice implanted with MC38 tumors expressing the LCMV glycoprotein (Fig. S13A). We observed a delay in tumor growth in mice that received Tpex bound by αCD28 agonistic antibodies compared to control Tpex (Fig. S13B), suggesting that enhancing CD28 costimulation improves differentiation/functionality of Tpex progeny. However, the delay in tumor growth observed with transfer of CD28-costimulated Tpex did not ultimately result in increased survival (Fig. S13C), most likely due to the single and low dose adoptive transfer (10,000 Tpex).

To assess the effects of increasing CD28 signaling in Tpex differentiation in vivo, we sorted Tpex from LCMV chronically infected mice, with and without adding agonistic αCD28. Control CD28-untouched Tpex or Tpex bound by αCD28 agonistic antibodies were labeled with CTV and transferred into infection-matched recipient mice (Fig. 5A). Two weeks post-transfer, we found a higher frequency of donor CD45.2^{+} cells in the spleens of mice that received Tpex bound by αCD28 antibody (Fig. 5B and C), indicating that enhanced CD28 signaling resulted in superior expansion. Tpex stimulated with αCD28 also generated a higher frequency of CD39^{+} PD-1^{+} CTV^{low} cells (Fig. 5D). CD39^{+} PD-1^{+} Tex are heterogenous and among these cells, a population of more functional “transitional” *effector-like* Tex can be identified by the expression of the chemokine receptor CX3CR1 (20, 21).

In control CD28-untouched Tpex, only a low frequency of CX3CR1^{+} *effector-like* cells was observed (Fig. 5E), consistent with the low frequency of *effector-like* cells observed in mice with helpless life-long chronic LCMV infection (20, 21) (Fig. 5E). However, Tpex stimulated with agonistic αCD28 gave rise to a substantial number of CX3CR1^{+} TCF-1^{neg} *effector-like* cells (Fig. 5E and F). Together these data suggest that enhancing CD28 signaling can improve functionality of PD-1^{+} CD8 T cells.

A critical question on PD-1^{+} CD8 T cell modulation is whether differentiation would diminish the Tpex pool and thus compromise long-term responses. To assess if enhancing CD28 costimulation would negatively impact self-renewal, we investigated the ability of CD28-stimulated Tpex cells to proliferate (CTV^{low}) while retaining their progenitor state (TCF-1^{+}) (Fig. 5G). We observed similar numbers of CTV^{low} and total TCF-1^{+} donor cells after transfer of control Tpex or CD28-stimulated Tpex (Fig. 5H), demonstrating that enhancing CD28 signaling does not prevent Tpex self-renewal, at least in this experimental setup and short-term analysis after two weeks. Overall, our findings support the concept that enhancing CD28 costimulation during chronic stimulation promotes Tpex differentiation and reinvigoration of antigen-specific CD8 T cells, and it may not compromise longevity of responses.

DISCUSSION

Maintenance of PD-1^{+} CD8 T cells exposed to persistent TCR stimulation is supported by Tpex that undergo slow homeostatic self-renewal as well as differentiation to give rise to cells with residual effector function (1, 3–6). Yet, cellular interactions and molecular pathways that regulate Tpex self-renewal and differentiation are not well understood. Here we show that CD28 signaling controls Tpex self-renewal and differentiation and our data suggest that CD28 may control Tpex fate through metabolic regulation. Sustained CD28 signaling on Tpex was necessary to maintain mitochondrial fitness and long-term maintenance of T cell responses. Furthermore, we demonstrate that whereas low levels of CD28 costimulation are sufficient to promote oxidative phosphorylation and Tpex self-renewal, stronger CD28 signaling induced a glycolytic switch and was necessary for Tpex conversion into Tex with effector-like function (Fig. S14).

Mitochondrial fitness is a requirement for T cell function and mitochondrial dysfunction contributes to the development of T cell exhaustion (25, 35, 36). Tpex display a more favorable metabolic state than the bulk of exhausted T cells (26). Similar to memory T cells (37), it was recently shown that preserved mitochondrial fitness and OXPHOS capacity allow Tpex to maintain functionality and long-term survival (26, 36). Our data reveal a central role of CD28 costimulation in the maintenance of Tpex metabolism. Both the loss of CD28 expression by Tpex and B7 blockade resulted in reduced Tpex OXPHOS capacity and also prevented long-term maintenance of anti-viral CD8 T cell responses during chronic LCMV infection. These correlative results have important implications for understanding the specific conditions/niches that are necessary to support Tpex survival and longevity of CD8 T cell responses during persistent antigen stimulation. Our data provide a likely mechanistic insight into the importance of Tpex interactions with B7-expressing APCs, such as dendritic cells (DCs).

Mechanistically, we show that costimulation continues to shape T cell responses beyond the priming phase: CD28 signaling enhances Tpex glycolytic activity in a dose-dependent manner and results in upregulation of IRF4. IRF4 expression is tightly regulated by TCR signaling strength (34, 38) but was also recently shown to be fine-tuned by CD28 signaling in plasma cells (39). IRF4 is a key factor in T cell differentiation, and different concentrations of IRF4 activate distinct transcriptional programs due to variable affinity of enhancers (40). Furthermore, IRF4 expression levels have been shown to dictate the amount of aerobic glycolysis and effector function in CD8 T cells (34, 41). Thus, we propose that Tpex require strong CD28 signaling to achieve sufficient levels of IRF4 expression and glycolytic commitment for differentiation. These data suggest that APCs with high expression of CD28 ligands would be responsible for Tex conversion. The data presented here are in line with correlative studies in cancer patients that show that Tpex-APC proximity in the tumor microenvironment is associated with differentiation and expansion of PD-1$^+$ CD8 T cells (9, 12, 42).

We propose that strong CD28 costimulation is required to promote conversion of Tpex into *effector-like* Tex. Although Tpex express much higher levels of CD28 than more differentiated Tex, and thus we focused on the role of CD28 on Tpex, it is conceivable that CD28 signaling may also play a role in maintaining functionality of *effector-like* Tex. Our previous work revealed a requirement for CD28 costimulation for effective PD-1 therapy (17), and biochemical studies demonstrated that PD-1 inhibits CD28 signaling (43). Hence blockade of the PD-1 pathway would enhance CD28 signaling when PD-1$^+$ CD8 T cells interact with B7-expressing APCs. In accordance with this hypothesis, recent work demonstrated that polyfunctional PD-1$^+$ CD8 T cells in human ovarian cancer are located in intraepithelial myeloid APC niches that provide CD28 costimulation to T cells during PD-1 blockade therapy (18). These observations are consistent with additional studies that have shown the importance of DCs for effective PD-1 targeted therapy (44–46). Furthermore, our recent data in hepatocellular carcinoma show that in tumors that respond to PD-1 blockade, Tpex are in close proximity to CXCL13$^+$ helper CD4 T cells and DCs enriched in maturation (e.g. high expression of B7 ligands) and immunoregulatory molecules (e.g. PD-L1), described as mregDCs (12). In addition, responder patients also presented a higher number of effector-like Tex in the tumor microenvironment, suggesting that Tpex interactions with CD4 helpers and mregDCs may promote effective Tex differentiation. Overall, our data support combining PD-1 targeted immunotherapy with strategies that promote DC recruitment and activation to enhance anti-tumor immune responses.

CD4 helper cells enhance priming of naïve CD8 T cells and are essential for optimal responses during acute infections or vaccinations (47). CD4 T cells can license professional APCs (48, 49) and provide direct help to CD8 T cells via cytokines (20, 50). In humans, CD4-help is critical for hepatitis C virus (HCV) control, and poor CD4 T cell responses are associated with chronic HCV infection (51, 52). Likewise, lack of CD4-help results in life-long chronic infection in a mouse model of HCV and with LCMV (19, 53). Transient CD4 depletion before LCMV infection results in high and sustained viremia, accompanied by severe CD8 T cell exhaustion, with lower frequency of effector-like PD-1$^+$ CD8 T cells (19, 20). Here, we assessed the role of the CD28/B7 pathway for sustaining PD-1$^+$ CD8 T cell responses in both helped and unhelped environments, and we found similar requirements for

CD28 costimulation. Nevertheless, our study did not address whether alternative therapeutic strategies, such as cytokine administration or metabolic modulation, could overcome the need for CD28 costimulation.

Strategies that engage CD28 are being developed to improve anti-tumor immunotherapy. For example, bispecific antibodies that target CD28 and tumor-specific antigens (TSA) synergize with anti-CD3/TSA bispecific and/or PD-1 targeted therapy (54, 55). Similarly, tri-specific CD3/CD28/TSA antibodies have also been evaluated with positive results in vitro and in animal models (56). These therapeutics have been modified to reduce binding to Fcγ receptors and restrict CD28 signaling to T cells interacting with tumor cells and thus have had, so far, a good safety profile in mice and non-human primates (54–56). Although our study did not evaluate the impact of strong and sustained CD28 signaling on Tpex, the data presented here provide reassurance that it is possible to enhance differentiation into more effective T cells by CD28 pathway engagement without draining the progenitor Tpex population and compromising longevity of responses. This is consistent with data from Gill *et al.* showing that blockade of the PD-1/PD-L1 pathway, which enhances CD28 signaling (43), not only improved Tpex differentiation into *effector-like* Tex but also increased their self-renewal (57).

Overall, our data reveal a central role of CD28 costimulation in preserving Tpex metabolic fitness. Continuous CD28 stimulation is required to maintain PD-1$^+$ CD8 T cell responses. Low levels of CD28 signaling are sufficient to maintain mitochondrial oxidative phosphorylation and self-renewal of Tpex. However, stronger CD28 signaling is needed to engage glycolysis, increase IRF4 expression and promote Tpex conversion into Tex that retain effector function (Fig. S14). Yet, enhancing CD28 signaling did not reduce Tpex self-renewal. These findings have important implications for immunotherapy in cancer and other situations of persistent T cell stimulation, such as chronic infections and autoimmunity.

MATERIALS AND METHODS

Study design:

The aim of this study is to address the function of CD28 costimulation for PD-1$^+$ CD8 T cells during chronic antigen stimulation. We used an in vivo mouse model of chronic infection with lymphocytic choriomenenigtis virus. Depletion of CD4 T cells prior to infection was performed in most experiments, as indicated, to ensure stable viral load and life-long infection. We prevented CD28 signaling by (1) blocking CD28 ligands with antibodies; (2) inducible *Cd28* deletion by tamoxifen administration to CD28^{flox} Cre-ERT2 mice or WT mice that received transfer of CD28^{flox} Cre-ERT2 cells, as indicated. No data were excluded from the study. Before antibodies or tamoxifen injection, mice were randomized based on their virus-specific cell frequency in blood to ensure comparable groups prior to treatment. Transfer experiments were used to determine how CD28 levels modulate fate of progenitor exhausted CD8 T cells. Flow cytometry was used to characterize the phenotype and functionality of virus-specific T cells. Bulk RNA-sequencing and seahorse assays were used to evaluate CD28-related transcriptional and metabolic regulation. Electron microscopy images were analyzed blindly by external collaborators. Sampling replicates and number of animals are indicated in figure legends.

Mice and infections:

C57BL/6J (B6, stock 000664), congenic B6 CD45.1 (B6.SJL-*Ptprc*^{a} *Pepc*^{b}/BoyJ, stock 002014), CD28KO (stock 002667) and Rosa26Cre-ERT2 (stock 008463) mice were purchased from the Jackson Laboratory. CD45.1 P14 TCR transgenic mice (58) (TCR for the H2-D^{b}-restricted LCMV glycoprotein epitope GP33) were bred in house. Rosa26Cre-ERT2 mice were bred in house to CD45.1 P14 TCR transgenic mice and *Cd28*$^{f/f}$ mice (59), gifted by Dr. Laurence A. Turka. Mice were infected at 6–8 weeks of age. Both males and females were used for experiments, with no noted sex-differences. For acute LCMV infection, mice were given 2×10^{5} plaque forming units (PFU) LCMV Armstrong (Arm) intraperitoneally (i.p.). For life-long chronic LCMV infection, the helpless model was used, unless otherwise indicated (19): mice were given 200 μg of the CD4-depleting antibody GK1.5 i.p. (BioXcell) 1 day prior to infection and again on the day of infection with 2×10^{6} PFU LCMV clone 13 by intravenous route (i.v.). For helped LCMV infection, mice were infected with 2×10^{6} PFU LCMV clone 13 i.v.. Mice received further treatments once chronic infection was established (at least 40 days post-infection), unless otherwise noted. Viral load was assessed by plaque assays on Vero E6 cells as previously described (60). All animal experiments performed in this study were approved by the Institutional Animal Care and Use Committee of Icahn School of Medicine at Mount Sinai (protocol number IACUC-2018–0018/ PROTO201900610).

Adoptive cell transfers:

For experiments analyzing P14 T cells, CD8 T cells were enriched from splenocytes from naïve P14 mice with the EasySep Mouse CD8 T Cell Isolation Kit (StemCell). 2×10^{3} P14 CD8 T cells were transferred i.v. into B6 recipient mice one day before infection with LCMV clone 13. In P14 cotransfer experiments, either *Cd28*$^{fl/fl}$ CreERT2^{neg} or *Cd28*$^{wt/wt}$ CreERT2^{+} cells were used as controls with similar results.

For Tpex transfer experiments, splenocytes were isolated from LCMV clone 13 infected mice at least 40 days post-infection (and 2–3 weeks post tamoxifen administration as indicated). Spleens were digested for 30 minutes at 37°C with 0.4 U/ml of collagenase D (Roche, # 11088882001). After CD8 enrichment (StemCell), 20×10^{6} cells were labeled with 5 μM cell trace violet (CTV, Thermo Fisher Scientific) during 20min at 37°C. CTV staining was quenched for 5 min with RPMI containing 10% FBS before proceeding with cell surface staining with anti-CD8α (53–6.7), -CD44 (IM7), -CD28 (E18), -CD39 (24DMS1) and -PD-1 (RMP1–30; non-blocking clone) from BD or Biolegend and Live/Dead fixable dead cell stain (Invitrogen). Live CD8^{+} PD-1^{+} CD39^{neg} Tpex were isolated by FACS (post-sort purity >96%) and 1×10^{5} cells were transferred i.v. to infection matched CD45.1^{+} mice. 2–5 weeks post-transfer, single cell suspensions were obtained from spleen and lung for staining and analysis.

Ex vivo Tpex culture:

Between $0.75–1\times10^{5}$ CTV-labelled sorted Tpex were stimulated with 3μg/ml αCD3-biotin (145–2C11, Thermo Fisher) crosslinked with 1.5μg/ml streptavidin (Anaspec) and variable amount of soluble αCD28 (37.51, Biolegend, 0.05 or 2μg/ml) and cultured for 5 days before analysis.

In vivo treatments:

For blockade of B7 molecules, 200 μg anti-mouse B7–1 (16–10A1, BioXcell) and 200 μg anti-mouse B7–2 (GL-1, BioXcell) were administered i.p. every 3 days. Control mice were left untreated or received 200 μg Rat IgG2a and 200 μg polyclonal Armenian Hamster IgG i.p. every 3 days. We obtained similar data when mice received isotype control antibodies or were untreated. Final analyses were performed 2–7 weeks after treatment initiation as indicated.

In vivo conditional *Cd28* gene deletion was achieved in $CD28^{fl/fl}$ Cre-ERT2 cells by tamoxifen administration. Tamoxifen (Sigma-Aldrich) was dissolved in ethanol, diluted 1:20 in sunflower oil, and sonicated for 5 min at 37°C. Mice were injected daily i.p. with 1 mg tamoxifen i.p. for 5 consecutive days, then rested for a minimum of 7 days before further analysis or treatment. We obtained about 50% efficiency of *Cd28* deletion and thus phenotypic characterization or cell sorting was performed after gating on $CD28^{neg}$ as described, but in Fig. 2A–F and S5 the entire P14 T cell population (heterozygous $Cd28^{fl/wt}$ $CreERT2^{+}$ or homozygous $Cd28^{fl/fl}$ $CreERT2^{+}$), not gated based on CD28 expression, was evaluated and compared to control $CreERT2^{neg}$ P14 T cells.

Antibodies and flow cytometry:

Single cell suspensions were obtained from blood, spleen, lung and liver as previously described (29). Prior to surface staining, cells were incubated with fixable viability dye (Thermofisher) for 10 min on ice. Single cell suspensions were then surface stained for 30 min on ice in flow cytometry buffer (PBS, 2% FBS, 1mM EDTA, 0.05% sodium azide) with the following antibodies recognizing: CD8a (53–6.7), PD-1 (29F.1A12), CD28 (E18), TIM-3 (RMT3–23), CD101 (Moushi101), CX3CR1 (SA011F11), CD73 (TY/11.8), ICOS (15F9), CD39 (24DMS1), CD44 (IM7), CD4 (RM4–5), CD45.2 (104), CD45.1 (A20) from BD, eBioscience or Biolegend (Table S1). LCMV-derived Db/GP33–41 and Db/GP276–286 biotinylated monomers were obtained from NIH tetramer core facility, tetramerized as previously described (61) and used for staining together with surface antibodies. Intracellular cytokine staining was performed after restimulation of splenocytes with 0.1 μg/ml of GP33 LCMV peptide in the presence of GolgiPlug (brefeldin A) and GolgiStop (monensin) for 5h at 37°C. Intracellular staining for IFN-γ (XMG1.2), TNF-α (MP6-XT22), and XCL-1 (polyclonal) was performed with Cytofix/Cytoperm kit (BD Biosciences) or Foxp3/ Transcription Factor Staining Buffer Set (eBioscience) if cytokines and transcription factors were co-stained. Secondary anti-Goat-FITC (Jackson Immunoresearch) was used 30 min at room temperature to detect anti-XCL-1 primary antibody. Intracellular transcription factor staining was performed with Foxp3/ Transcription Factor Staining Buffer Set (eBioscience) according to the manufacturer's instructions with the following antibodies: TCF-1 (C63D9 and S33–966), Bcl6 (IG191E/A8), IRF4 (3E4), Tbet (4B10), TOX (REA473). Intracellular staining for Ki-67 (B56) and granzyme B (GB11) was also performed with Foxp3/ Transcription Factor Staining Buffer Set (eBioscience). Apoptosis was assessed after restimulation of splenocytes with 0.1 μg/ml of GP33 LCMV peptide for 4h at 37°C. Intracellular active caspase-3 (C92–605, BD Biosciences) staining was performed with Cytofix/Cytoperm kit (BD Biosciences).

Extracellular flux analysis:

Seahorse XFp sensor cartridges were hydrated overnight with Agilent Seahorse XF Calibrant. 60–75×10^3 cells were plated per well in Seahorse XF DMEM pH 7.4 supplemented with 1mM pyruvate, 2mM glutamine and 10mM glucose into Seahorse XF HS PDL miniplates. Cells were rested between 45–60min at 37°C in a non-CO_2 incubator before the assay on Seahorse XF HS Mini (Agilent).

Mito Stress assay (Cell Mito Stress Test Kit, Agilent) was performed according to the manufacturer's instructions. Extracellular acidification (ECAR) and oxygen consumption rates (OCR) in response to oligomycin (2μM), FCCP (1μM) and Rotenone+Antimycin (0.5μM) were measured with Agilent Seahorse XF HS Mini Analyzer. Spare respiratory capacity (SRC) is measured as the difference between basal OCR values and maximal OCR values obtained after FCCP uncoupling.

For glycolysis (Glycolytic Rate Assay Kit, Agilent), after basal ECAR measurements were taken, T cells were stimulated with 3μg/ml αCD3-biotin (145–2C11, Thermo Fisher) crosslinked with 1.5μg/ml streptavidin (Anaspec) and soluble αCD28 (clone 37.51, Biolegend, 2μg/ml) for 1 hour (62). Then cells were treated with Rotenone+Antimycin (0.5μM) and 2-deoxy-D-glucose (2-DG) (50mM). Maximum ECAR post-stimulation (=ECAR maximum after αCD3/αCD28 stimulation and before Rot/AA treatment), glycolytic reserve (=difference between the compensatory glycolysis and ECAR pre-Rot/AA treatment) and compensatory glycolysis (=difference between basal ECAR values and maximal ECAR values measured after Rot/AA treatment) were determined.

Flow-based metabolic assays:

For the 2-NBDG uptake assay, splenocytes, from chronically infected mice where P14 T cells had been transferred, were plated at 1×10^6 cells per well in fully supplemented media (RPMI 10% FBS, 2mM L-glutamine, 10mM HEPES, 55μM β-mercaptoethanol, 100U/ml penicillin, 100μg/ml streptomycin). Cells were stimulated for 6 hours with GP33 peptide (1 nM), alone or in combination with agonistic αCD28 2μg/ml. In the last 30 minutes of stimulation, media was replaced by fully supplemented RPMI + 100μg/ml 2-NBDG (Thermofisher).

Mitochondrial ROS production was measured with MitoSOX (Thermo Fisher) according to manufacturer's instructions. Briefly, 2×10^6 cells were incubated in Hank's balanced salt solution (HBSS) with calcium and magnesium and MitoSOX (1μM) for 20 minutes at 37°C. After incubation cells were washed twice in flow cytometry buffer, surface stained with antibodies for 20 min on ice. Fluorescence was acquired immediately after surface staining was performed.

Bulk RNA-Sequencing:

10,000 cells were FACS sorted into lysis reagent (QIAGEN). After addition of chloroform (Sigma) and centrifugation, RNA was isolated from the aqueous phase using RNEasy Micro kit (QIAGEN). 1 ng RNA was used as input for the NEBNext Single Cell/Low Input RNA Library Prep Kit for Illumina (NEB). Poly-A enriched libraries were sequenced in 75bp

single-end mode on a NextSeq 500 system (Illumina) in the ISMMS NGS sequencing cores in the Department of Oncological Sciences. Reads were quasi-mapped to the Gencode M25 (GRCm38.p6) gene set using *salmon* (63) and differential gene expression analysis was performed between $CD28^{neg}$ and $CD28^{+}$ $CD73^{+}$ $CD39^{neg}$ P14 Tpex using *DESeq2* (64) after integrating the library preparation batch in the design matrix. Independent hypothesis weighting (IHW) was performed on p-values with the default covariate parameter of mean counts of each gene and significance level of 0.05 for FDR control (65). Significant genes were retained by filtering for an adjusted p-value < 0.05 and a log2 fold change > 0.75 or < −0.75. Gene set enrichment analysis was performed with the *fgsea* package (66) on the entire expressed gene set pre-ranked based on the Wald test statistic computed by DESeq2, significant pathways were reported using an adjusted P-value cutoff of 0.05 and ordered by normalized enrichment score. For heatmaps, the Z-score was calculated as (sample TPM - mean of all TPM) divided by standard deviation. Out of 5 Tpex samples used for DESeq2 analysis, only the 3 samples sequenced at the same time as the Tex samples are shown.

Electron microscopy:

After sorting specific CD8 T cell subpopulations, pellets of $100–200\times10^3$ cells were overlaid with 1ml fixative solution (4% PFA, 2.5% glutaraldehyde, 0.02% picric acid in 0.1M sodium cacodylate buffer), spun to a pellet and held overnight at 4°C. The cells were then washed with 0.1M Na-cacodylate buffer then post-fixed with 1% OsO4 −1.5% K-ferricyanide for 1h at RT. Washed cells were dehydrated by successive ethanol baths (50%, 75%, 85%, 95%, 3×100%) each of 15 mins, followed by transition through acetonitrile. Infiltration was performed with graduated steps of acetonitrile: epoxy resin, finishing with pure Embed812 epoxy resin. Samples were then embedded in fresh resin and polymerized at 50°C 36 hr. Ultrathin sections (65 nm) were contrasted with 1.5% aqueous uranyl acetate and then lead citrate (67) and viewed on a JEM 1400 electron microscope (JEOL, USA, Inc., Peabody, MA) operated at 100 kV. Digital images were captured on a Veleta 2K x 2K CCD camera (Olympus-SIS, Germany) and analyzed blindly by an independent expert. Cristae width was measured using ImageJ software and averaged over 90 independent images (around 800–1000 cristae per condition).

In vivo tumor model:

C57Bl/6 mice were inoculated subcutaneously with 0.5×10^6 MC38 colon adenocarcinoma cells expressing the LCMV glycoprotein (MC38-GP; pLVX-LCMV-GP vector used to modify MC38 cells was a kind gift from Dr. Andreas Wieland, MC38 cells were obtained from Dr. Nicholas Restifo). The same day, mice also received 10×10^3 intravenous Tpex ($CD8^{+}$ $PD\text{-}1^{+}$ $CD39^{neg}$) sorted from life-long LCMV chronically infected mice with or without anti-CD28 (E18) antibody. Tumors were measured every 2–3 days using a caliper, and tumor growth was calculated as volume of ellipsoid (length x width x width x 0.52). Mice whose tumors exceeded acceptable limits (1000 mm^3 or ulcerated tumors) were euthanized.

Statistical analysis:

Comparisons between two groups were performed with an unpaired *t* test for independent samples, or a paired *t* test for paired samples. For multiple comparisons, one-way analysis

of variance (ANOVA) with Sidak's correction was used. Non-parametric tests were used when data did not fit normal distribution, using Mann Whitney tests for the comparison of two groups, or Kruskall-Wallis Dun's corrected for multiple group comparison for more than two groups. Unless otherwise noted, symbols represent individual mice and error bars indicate standard error of the mean (SEM). When possible, data from all experiments are shown. Data were analyzed using Prism 7 (Graphpad) and the specific statistic tests used are listed in each figure.

Supplementary Material

Refer to Web version on PubMed Central for supplementary material.

Acknowledgments:

We thank the NIH Tetramer Core Facility, Center for Comparative Medicine and Surgery, Mitochondrial Analysis Facility, Dean's Flow Cytometry CORE and Oncological Sciences Sequencing Core at the Icahn School of Medicine at Mount Sinai (ISMMS). We thank J. Jimenez for technical assistance, and the Electron Microscopy & Histology services of the Weill Cornell Medicine Microscopy & Image Analysis Core. We thank L.A. Turka for $CD28^{f/f}$ mice and R. Ahmed for P14 mice. We thank A.V. Menk and G.M. Delgoffe from University of Pittsburgh for advice and protocols regarding T cell stimulation for metabolic assays.

Funding:

Funding was provided by the NIH (R01 AI153363-01A1 to AOK, EH and JL; R33 CA263705-01 to MES and ZHG; and R01CA154683 to EB and DF). EH was supported by the Philippe Foundation. The Oncological Sciences Sequencing Core was supported by Tisch Cancer Institute, Cancer Center Support Grant P30 CA196521.

AOK receives research support from Merck and has served as a consultant for AstraZeneca and Axon Advisors.

Data and materials availability:

Raw data from RNA-seq experiments have been deposited at GEO, accession number GSE200506. All reagents generated in this study are available from the Lead Contact. All data needed to evaluate the conclusions in the paper are present in the paper or the Supplementary Materials.

References and Notes

1. Hashimoto M, Kamphorst AO, Im SJ, Kissick HT, Pillai RN, Ramalingam SS, Araki K, Ahmed R, CD8 T Cell Exhaustion in Chronic Infection and Cancer: Opportunities for Interventions. Annu Rev Med 69, 301–318 (2018). [PubMed: 29414259]
2. McLane LM, Abdel-Hakeem MS, Wherry EJ, CD8 T Cell Exhaustion During Chronic Viral Infection and Cancer. Annu Rev Immunol 37, 457–495 (2019). [PubMed: 30676822]
3. Wu T, Ji Y, Moseman EA, Xu HC, Manglani M, Kirby M, Anderson SM, Handon R, Kenyon E, Elkahloun A, Wu W, Lang PA, Gattinoni L, McGavern DB, Schwartzberg PL, The TCF1-Bcl6 axis counteracts type I interferon to repress exhaustion and maintain T cell stemness. Sci Immunol 1, eaai8593 (2016).
4. Utzschneider DT, Charmoy M, Chennupati V, Pousse L, Ferreira DP, Calderon-Copete S, Danilo M, Alfei F, Hofmann M, Wieland D, Pradervand S, Thimme R, Zehn D, Held W, T Cell Factor 1-Expressing Memory-like CD8(+) T Cells Sustain the Immune Response to Chronic Viral Infections. Immunity 45, 415–427 (2016). [PubMed: 27533016]
5. He R, Hou S, Liu C, Zhang A, Bai Q, Han M, Yang Y, Wei G, Shen T, Yang X, Xu L, Chen X, Hao Y, Wang P, Zhu C, Ou J, Liang H, Ni T, Zhang X, Zhou X, Deng K, Chen Y, Luo Y, Xu J, Qi H, Wu

Y, Ye L, Follicular CXCR5- expressing CD8(+) T cells curtail chronic viral infection. Nature 537, 412–428 (2016). [PubMed: 27501245]

6. Im SJ, Hashimoto M, Gerner MY, Lee J, Kissick HT, Burger MC, Shan Q, Hale JS, Nasti TH, Sharpe AH, Freeman GJ, Germain RN, Nakaya HI, Xue HH, Ahmed R, Defining CD8+ T cells that provide the proliferative burst after PD-1 therapy. Nature 537, 417–421 (2016). [PubMed: 27501248]
7. Miller BC, Sen DR, Al Abosy R, Bi K, Virkud YV, LaFleur MW, Yates KB, Lako A, Felt K, Naik GS, Manos M, Gjini E, Kuchroo JR, Ishizuka JJ, Collier JL, Griffin GK, Maleri S, Comstock DE, Weiss SA, Brown FD, Panda A, Zimmer MD, Manguso RT, Hodi FS, Rodig SJ, Sharpe AH, Haining WN, Subsets of exhausted CD8(+) T cells differentially mediate tumor control and respond to checkpoint blockade. Nat Immunol 20, 326–336 (2019). [PubMed: 30778252]
8. Siddiqui I, Schaeuble K, Chennupati V, Fuertes Marraco SA, Calderon-Copete S, Pais Ferreira D, Carmona SJ, Scarpellino L, Gfeller D, Pradervand S, Luther SA, Speiser DE, Held W, Intratumoral Tcf1(+)PD-1(+)CD8(+) T Cells with Stem-like Properties Promote Tumor Control in Response to Vaccination and Checkpoint Blockade Immunotherapy. Immunity 50, 195–211 e110 (2019). [PubMed: 30635237]
9. Jansen CS, Prokhnevska N, Master VA, Sanda MG, Carlisle JW, Bilen MA, Cardenas M, Wilkinson S, Lake R, Sowalsky AG, Valanparambil RM, Hudson WH, McGuire D, Melnick K, Khan AI, Kim K, Chang YM, Kim A, Filson CP, Alemozaffar M, Osunkoya AO, Mullane P, Ellis C, Akondy R, Im SJ, Kamphorst AO, Reyes A, Liu Y, Kissick H, An intra-tumoral niche maintains and differentiates stem-like CD8 T cells. Nature 576, 465–470 (2019). [PubMed: 31827286]
10. Sade-Feldman M, Yizhak K, Bjorgaard SL, Ray JP, de Boer CG, Jenkins RW, Lieb DJ, Chen JH, Frederick DT, Barzily-Rokni M, Freeman SS, Reuben A, Hoover PJ, Villani AC, Ivanova E, Portell A, Lizotte PH, Aref AR, Eliane JP, Hammond MR, Vitzthum H, Blackmon SM, Li B, Gopalakrishnan V, Reddy SM, Cooper ZA, Paweletz CP, Barbie DA, Stemmer-Rachamimov A, Flaherty KT, Wargo JA, Boland GM, Sullivan RJ, Getz G, Hacohen N, Defining T Cell States Associated with Response to Checkpoint Immunotherapy in Melanoma. Cell 176, 404 (2019). [PubMed: 30633907]
11. Eberhardt CS, Kissick HT, Patel MR, Cardenas MA, Prokhnevska N, Obeng RC, Nasti TH, Griffith CC, Im SJ, Wang X, Shin DM, Carrington M, Chen ZG, Sidney J, Sette A, Saba NF, Wieland A, Ahmed R, Functional HPV-specific PD-1(+) stem-like CD8 T cells in head and neck cancer. Nature 597, 279–284 (2021). [PubMed: 34471285]
12. Magen A, Hamon P, Fiaschi N, Soong BY, Park MD, Mattiuz R, Humblin E, Troncoso L, D'souza D, Dawson T, Kim J, Hamel S, Buckup M, Chang C, Tabachnikova A, Schwartz H, Malissen N, Lavin Y, Soares-Schanoski A, Giotti B, Hegde S, Ioannou G, Gonzalez-Kozlova E, Hennequin C, Le Berichel J, Zhao Z, Ward SC, Fiel I, Kou B, Dobosz M, Li L, Adler C, Ni M, Wei Y, Wang W, Atwal GS, Kundu K, Cygan KJ, Tsankov AM, Rahman A, Price C, Fernandez N, He J, Gupta NT, Kim-Schulze S, Gnjatic S, Kenigsberg E, Deering RP, Schwartz M, Marron TU, Thurston G, Kamphorst AO, Merad M, Intratumoral dendritic cell–CD4+ T helper cell niches enable CD8+ T cell differentiation following PD-1 blockade in hepatocellular carcinoma. Nature Medicine 29, 1389–1399 (2023).
13. Abdelsamed HA, Zebley CC, Nguyen H, Rutishauser RL, Fan Y, Ghoneim HE, Crawford JC, Alfei F, Alli S, Ribeiro SP, Castellaw AH, McGargill MA, Jin H, Boi SK, Speake C, Serti E, Turka LA, Busch ME, Stone M, Deeks SG, Sekaly RP, Zehn D, James EA, Nepom GT, Youngblood B, Beta cell-specific CD8(+) T cells maintain stem cell memory-associated epigenetic programs during type 1 diabetes. Nat Immunol 21, 578–587 (2020). [PubMed: 32231298]
14. Gearty SV, Dundar F, Zumbo P, Espinosa-Carrasco G, Shakiba M, Sanchez-Rivera FJ, Socci ND, Trivedi P, Lowe SW, Lauer P, Mohibullah N, Viale A, DiLorenzo TP, Betel D, Schietinger A, An autoimmune stem-like CD8 T cell population drives type 1 diabetes. Nature 602, 156–161 (2022). [PubMed: 34847567]
15. Im SJ, Konieczny BT, Hudson WH, Masopust D, Ahmed R, PD-1+ stemlike CD8 T cells are resident in lymphoid tissues during persistent LCMV infection. Proc Natl Acad Sci U S A 117, 4292–4299 (2020). [PubMed: 32034098]
16. Prokhnevska N, Cardenas MA, Valanparambil RM, Sobierajska E, Barwick BG, Jansen C, Reyes Moon A, Gregorova P, delBalzo L, Greenwald R, Bilen MA, Alemozaffar M, Joshi S, Cimmino C,

Larsen C, Master V, Sanda M, Kissick H, CD8(+) T cell activation in cancer comprises an initial activation phase in lymph nodes followed by effector differentiation within the tumor. Immunity 56, 107–124 e105 (2023). [PubMed: 36580918]

17. Kamphorst AO, Wieland A, Nasti T, Yang S, Zhang R, Barber DL, Konieczny BT, Daugherty CZ, Koenig L, Yu K, Sica GL, Sharpe AH, Freeman GJ, Blazar BR, Turka LA, Owonikoko TK, Pillai RN, Ramalingam SS, Araki K, Ahmed R, Rescue of exhausted CD8 T cells by PD-1-targeted therapies is CD28-dependent. Science 355, 1423–1427 (2017). [PubMed: 28280249]
18. Duraiswamy J, Turrini R, Minasyan A, Barras D, Crespo I, Grimm AJ, Casado J, Genolet R, Benedetti F, Wicky A, Ioannidou K, Castro W, Neal C, Moriot A, Renaud-Tissot S, Anstett V, Fahr N, Tanyi JL, Eiva MA, Jacobson CA, Montone KT, Westergaard MCW, Svane IM, Kandalaft LE, Delorenzi M, Sorger PK, Farkkila A, Michielin O, Zoete V, Carmona SJ, Foukas PG, Powell DJ Jr., Rusakiewicz S, Doucey MA, Dangaj Laniti D, Coukos G, Myeloid antigen-presenting cell niches sustain antitumor T cells and license PD-1 blockade via CD28 costimulation. Cancer Cell 39, 1623–1642 e1620 (2021). [PubMed: 34739845]
19. Matloubian M, Concepcion RJ, Ahmed R, CD4+ T cells are required to sustain CD8+ cytotoxic T-cell responses during chronic viral infection. J Virol 68, 8056–8063 (1994). [PubMed: 7966595]
20. Zander R, Schauder D, Xin G, Nguyen C, Wu X, Zajac A, Cui W, CD4(+) T Cell Help Is Required for the Formation of a Cytolytic CD8(+) T Cell Subset that Protects against Chronic Infection and Cancer. Immunity 51, 1028–1042 e1024 (2019). [PubMed: 31810883]
21. Hudson WH, Gensheimer J, Hashimoto M, Wieland A, Valanparambil RM, Li P, Lin JX, Konieczny BT, Im SJ, Freeman GJ, Leonard WJ, Kissick HT, Ahmed R, Proliferating Transitory T Cells with an Effector-like Transcriptional Signature Emerge from PD-1. Immunity 51, 1043–1058.e1044 (2019). [PubMed: 31810882]
22. Li C, Zhu B, Son YM, Wang Z, Jiang L, Xiang M, Ye Z, Beckermann KE, Wu Y, Jenkins JW, Siska PJ, Vincent BG, Prakash YS, Peikert T, Edelson BT, Taneja R, Kaplan MH, Rathmell JC, Dong H, Hitosugi T, Sun J, The Transcription Factor Bhlhe40 Programs Mitochondrial Regulation of Resident CD8(+) T Cell Fitness and Functionality. Immunity 51, 491–507 e497 (2019). [PubMed: 31533057]
23. Bengsch B, Johnson AL, Kurachi M, Odorizzi PM, Pauken KE, Attanasio J, Stelekati E, McLane LM, Paley MA, Delgoffe GM, Wherry EJ, Bioenergetic Insufficiencies Due to Metabolic Alterations Regulated by the Inhibitory Receptor PD-1 Are an Early Driver of CD8(+) T Cell Exhaustion. Immunity 45, 358–373 (2016). [PubMed: 27496729]
24. Man K, Gabriel SS, Liao Y, Gloury R, Preston S, Henstridge DC, Pellegrini M, Zehn D, Berberich-Siebelt F, Febbraio MA, Shi W, Kallies A, Transcription Factor IRF4 Promotes CD8(+) T Cell Exhaustion and Limits the Development of Memory-like T Cells during Chronic Infection. Immunity 47, 1129–1141 e1125 (2017). [PubMed: 29246443]
25. Scharping NE, Menk AV, Moreci RS, Whetstone RD, Dadey RE, Watkins SC, Ferris RL, Delgoffe GM, The Tumor Microenvironment Represses T Cell Mitochondrial Biogenesis to Drive Intratumoral T Cell Metabolic Insufficiency and Dysfunction. Immunity 45, 374–388 (2016). [PubMed: 27496732]
26. Gabriel SS, Tsui C, Chisanga D, Weber F, Llano-Leon M, Gubser PM, Bartholin L, Souza-Fonseca-Guimaraes F, Huntington ND, Shi W, Utzschneider DT, Kallies A, Transforming growth factor-beta-regulated mTOR activity preserves cellular metabolism to maintain long-term T cell responses in chronic infection. Immunity 54, 1698–1714 e1695 (2021). [PubMed: 34233154]
27. Cogliati S, Frezza C, Soriano ME, Varanita T, Quintana-Cabrera R, Corrado M, Cipolat S, Costa V, Casarin A, Gomes LC, Perales-Clemente E, Salviati L, Fernandez-Silva P, Enriquez JA, Scorrano L, Mitochondrial cristae shape determines respiratory chain supercomplexes assembly and respiratory efficiency. Cell 155, 160–171 (2013). [PubMed: 24055366]
28. Klein Geltink RI, O'Sullivan D, Corrado M, Bremser A, Buck MD, Buescher JM, Firat E, Zhu X, Niedermann G, Caputa G, Kelly B, Warthorst U, Rensing-Ehl A, Kyle RL, Vandersarren L, Curtis JD, Patterson AE, Lawless S, Grzes K, Qiu J, Sanin DE, Kretz O, Huber TB, Janssens S, Lambrecht BN, Rambold AS, Pearce EJ, Pearce EL, Mitochondrial Priming by CD28. Cell 171, 385–397.e311 (2017). [PubMed: 28919076]
29. Buck MD, O'Sullivan D, Pearce EL, T cell metabolism drives immunity. J Exp Med 212, 1345–1360 (2015). [PubMed: 26261266]

30. Frauwirth KA, Riley JL, Harris MH, Parry RV, Rathmell JC, Plas DR, Elstrom RL, June CH, Thompson CB, The CD28 signaling pathway regulates glucose metabolism. Immunity 16, 769–777 (2002). [PubMed: 12121659]

31. Jacobs SR, Herman CE, Maciver NJ, Wofford JA, Wieman HL, Hammen JJ, Rathmell JC, Glucose uptake is limiting in T cell activation and requires CD28-mediated Akt-dependent and independent pathways. J Immunol 180, 4476–4486 (2008). [PubMed: 18354169]

32. Beckermann KE, Hongo R, Ye X, Young K, Carbonell K, Healey DCC, Siska PJ, Barone S, Roe CE, Smith CC, Vincent BG, Mason FM, Irish JM, Rathmell WK, Rathmell JC, CD28 costimulation drives tumor-infiltrating T cell glycolysis to promote inflammation. JCI Insight 5, e138729 (2020).

33. Sinclair LV, Barthelemy C, Cantrell DA, Single Cell Glucose Uptake Assays: A Cautionary Tale. Immunometabolism 2, e200029 (2020).

34. Man K, Miasari M, Shi W, Xin A, Henstridge DC, Preston S, Pellegrini M, Belz GT, Smyth GK, Febbraio MA, Nutt SL, Kallies A, The transcription factor IRF4 is essential for TCR affinity-mediated metabolic programming and clonal expansion of T cells. Nat Immunol 14, 1155–1165 (2013). [PubMed: 24056747]

35. Yu YR, Imrichova H, Wang H, Chao T, Xiao Z, Gao M, Rincon-Restrepo M, Franco F, Genolet R, Cheng WC, Jandus C, Coukos G, Jiang YF, Locasale JW, Zippelius A, Liu PS, Tang L, Bock C, Vannini N, Ho PC, Disturbed mitochondrial dynamics in CD8(+) TILs reinforce T cell exhaustion. Nat Immunol 21, 1540–1551 (2020). [PubMed: 33020660]

36. Vardhana SA, Hwee MA, Berisa M, Wells DK, Yost KE, King B, Smith M, Herrera PS, Chang HY, Satpathy AT, van den Brink MRM, Cross JR, Thompson CB, Impaired mitochondrial oxidative phosphorylation limits the self-renewal of T cells exposed to persistent antigen. Nat Immunol 21, 1022–1033 (2020). [PubMed: 32661364]

37. van der Windt GJ, Everts B, Chang CH, Curtis JD, Freitas TC, Amiel E, Pearce EJ, Pearce EL, Mitochondrial respiratory capacity is a critical regulator of CD8+ T cell memory development. Immunity 36, 68–78 (2012). [PubMed: 22206904]

38. Nayar R, Schutten E, Bautista B, Daniels K, Prince AL, Enos M, Brehm MA, Swain SL, Welsh RM, Berg LJ, Graded levels of IRF4 regulate CD8+ T cell differentiation and expansion, but not attrition, in response to acute virus infection. J Immunol 192, 5881–5893 (2014). [PubMed: 24835398]

39. Utley A, Chavel C, Lightman S, Holling GA, Cooper J, Peng P, Liu W, Barwick BG, Gavile CM, Maguire O, Murray-Dupuis M, Rozanski C, Jordan MS, Kambayashi T, Olejniczak SH, Boise LH, Lee KP, CD28 Regulates Metabolic Fitness for Long-Lived Plasma Cell Survival. Cell Rep 31, 107815 (2020). [PubMed: 32579940]

40. Iwata A, Durai V, Tussiwand R, Briseno CG, Wu X, Grajales-Reyes GE, Egawa T, Murphy TL, Murphy KM, Quality of TCR signaling determined by differential affinities of enhancers for the composite BATF-IRF4 transcription factor complex. Nat Immunol 18, 563–572 (2017). [PubMed: 28346410]

41. Seo H, Gonzalez-Avalos E, Zhang W, Ramchandani P, Yang C, Lio CJ, Rao A, Hogan PG, BATF and IRF4 cooperate to counter exhaustion in tumor-infiltrating CAR T cells. Nat Immunol 22, 983–995 (2021). [PubMed: 34282330]

42. Di Pilato M, Kfuri-Rubens R, Pruessmann JN, Ozga AJ, Messemaker M, Cadilha BL, Sivakumar R, Cianciaruso C, Warner RD, Marangoni F, Carrizosa E, Lesch S, Billingsley J, Perez-Ramos D, Zavala F, Rheinbay E, Luster AD, Gerner MY, Kobold S, Pittet MJ, Mempel TR, CXCR6 positions cytotoxic T cells to receive critical survival signals in the tumor microenvironment. Cell 184, 4512–4530 e4522 (2021). [PubMed: 34343496]

43. Hui E, Cheung J, Zhu J, Su X, Taylor MJ, Wallweber HA, Sasmal DK, Huang J, Kim JM, Mellman I, Vale RD, T cell costimulatory receptor CD28 is a primary target for PD-1-mediated inhibition. Science 355, 1428–1433 (2017). [PubMed: 28280247]

44. Salmon H, Idoyaga J, Rahman A, Leboeuf M, Remark R, Jordan S, Casanova-Acebes M, Khudoynazarova M, Agudo J, Tung N, Chakarov S, Rivera C, Hogstad B, Bosenberg M, Hashimoto D, Gnjatic S, Bhardwaj N, Palucka AK, Brown BD, Brody J, Ginhoux F, Merad M, Expansion and Activation of CD103(+) Dendritic Cell Progenitors at the Tumor Site Enhances

Tumor Responses to Therapeutic PD-L1 and BRAF Inhibition. Immunity 44, 924–938 (2016). [PubMed: 27096321]

45. Spranger S, Dai D, Horton B, Gajewski TF, Tumor-Residing Batf3 Dendritic Cells Are Required for Effector T Cell Trafficking and Adoptive T Cell Therapy. Cancer Cell 31, 711–723 e714 (2017). [PubMed: 28486109]
46. Chow MT, Ozga AJ, Servis RL, Frederick DT, Lo JA, Fisher DE, Freeman GJ, Boland GM, Luster AD, Intratumoral Activity of the CXCR3 Chemokine System Is Required for the Efficacy of Anti-PD-1 Therapy. Immunity 50, 1498–1512.e1495 (2019). [PubMed: 31097342]
47. Bevan MJ, Helping the CD8(+) T-cell response. Nat Rev Immunol 4, 595–602 (2004). [PubMed: 15286726]
48. Ferris ST, Durai V, Wu R, Theisen DJ, Ward JP, Bern MD, Davidson J. T. t., Bagadia P, Liu T, Briseno CG, Li L, Gillanders WE, Wu GF, Yokoyama WM, Murphy TL, Schreiber RD, Murphy KM, cDC1 prime and are licensed by CD4(+) T cells to induce anti-tumour immunity. Nature 584, 624–629 (2020). [PubMed: 32788723]
49. Cohen M, Giladi A, Barboy O, Hamon P, Li B, Zada M, Gurevich-Shapiro A, Beccaria CG, David E, Maier BB, Buckup M, Kamer I, Deczkowska A, Le Berichel J, Bar J, Iannacone M, Tanay A, Merad M, Amit I, The interaction of CD4(+) helper T cells with dendritic cells shapes the tumor microenvironment and immune checkpoint blockade response. Nat Cancer 3, 303–317 (2022). [PubMed: 35241835]
50. West EE, Jin HT, Rasheed AU, Penaloza-Macmaster P, Ha SJ, Tan WG, Youngblood B, Freeman GJ, Smith KA, Ahmed R, PD-L1 blockade synergizes with IL-2 therapy in reinvigorating exhausted T cells. J Clin Invest 123, 2604–2615 (2013). [PubMed: 23676462]
51. Grakoui A, Shoukry NH, Woollard DJ, Han JH, Hanson HL, Ghrayeb J, Murthy KK, Rice CM, Walker CM, HCV persistence and immune evasion in the absence of memory T cell help. Science 302, 659–662 (2003). [PubMed: 14576438]
52. Smyk-Pearson S, Tester IA, Klarquist J, Palmer BE, Pawlotsky JM, Golden-Mason L, Rosen HR, Spontaneous recovery in acute human hepatitis C virus infection: functional T-cell thresholds and relative importance of CD4 help. J Virol 82, 1827–1837 (2008). [PubMed: 18045940]
53. Billerbeck E, Wolfisberg R, Fahnoe U, Xiao JW, Quirk C, Luna JM, Cullen JM, Hartlage AS, Chiriboga L, Ghoshal K, Lipkin WI, Bukh J, Scheel TKH, Kapoor A, Rice CM, Mouse models of acute and chronic hepacivirus infection. Science 357, 204–208 (2017). [PubMed: 28706073]
54. Waite JC, Wang B, Haber L, Hermann A, Ullman E, Ye X, Dudgeon D, Slim R, Ajithdoss DK, Godin SJ, Ramos I, Wu Q, Oswald E, Poon P, Golubov J, Grote D, Stella J, Pawashe A, Finney J, Herlihy E, Ahmed H, Kamat V, Dorvilliers A, Navarro E, Xiao J, Kim J, Yang SN, Warsaw J, Lett C, Canova L, Schulenburg T, Foster R, Krueger P, Garnova E, Rafique A, Babb R, Chen G, Stokes Oristian N, Siao CJ, Daly C, Gurer C, Martin J, Macdonald L, MacDonald D, Poueymirou W, Smith E, Lowy I, Thurston G, Olson W, Lin JC, Sleeman MA, Yancopoulos GD, Murphy AJ, Skokos D, Tumor-targeted CD28 bispecific antibodies enhance the antitumor efficacy of PD-1 immunotherapy. Sci Transl Med 12, (2020).
55. Skokos D, Waite JC, Haber L, Crawford A, Hermann A, Ullman E, Slim R, Godin S, Ajithdoss D, Ye X, Wang B, Wu Q, Ramos I, Pawashe A, Canova L, Vazzana K, Ram P, Herlihy E, Ahmed H, Oswald E, Golubov J, Poon P, Havel L, Chiu D, Lazo M, Provoncha K, Yu K, Kim J, Warsaw JJ, Stokes Oristian N, Siao CJ, Dudgeon D, Huang T, Potocky T, Martin J, MacDonald D, Oyejide A, Rafique A, Poueymirou W, Kirshner JR, Smith E, Olson W, Lin J, Thurston G, Sleeman MA, Murphy AJ, Yancopoulos GD, A class of costimulatory CD28-bispecific antibodies that enhance the antitumor activity of CD3-bispecific antibodies. Sci Transl Med 12, eaba2325 (2020).
56. Wu L, Seung E, Xu L, Rao E, Lord DM, Wei RR, Cortez-Retamozo V, Ospina B, Posternak V, Ulinski G, Piepenhagen P, Francesconi E, El-Murr N, Beil C, Kirby P, Li A, Fretland J, Vicente R, Deng G, Dabdoubi T, Cameron B, Bertrand T, Ferrari P, Pouzieux S, Lemoine C, Prades C, Park A, Qiu H, Song Z, Zhang B, Sun F, Chiron M, Rao S, Radosevic K, Yang ZY, Nabel GJ, Trispecific antibodies enhance the therapeutic efficacy of tumor-directed T cells through T cell receptor costimulation. Nat Cancer 1, 86–98 (2020). [PubMed: 35121834]
57. Gill Wang, Lee Hudson, Ando Araki, Hu Wieland, Im Gavora, Medina Freeman, Hashimoto Reiner, Ahmed., PD-1 blockade promotes both effector differentiation and increased self-

renewal of stem-like CD8 T cells to maintain their numbers. Sci Immunol, (2023). 10.1126/sciimmunol.adg0539

58. Pircher H, Burki K, Lang R, Hengartner H, Zinkernagel RM, Tolerance induction in double specific T-cell receptor transgenic mice varies with antigen. Nature 342, 559–561 (1989). [PubMed: 2573841]
59. Zhang R, Huynh A, Whitcher G, Chang J, Maltzman JS, Turka LA, An obligate cell-intrinsic function for CD28 in Tregs. J Clin Invest 123, 580–593 (2013). [PubMed: 23281398]
60. Ahmed R, Salmi A, Butler LD, Chiller JM, Oldstone MB, Selection of genetic variants of lymphocytic choriomeningitis virus in spleens of persistently infected mice. Role in suppression of cytotoxic T lymphocyte response and viral persistence. J Exp Med 160, 521–540 (1984). [PubMed: 6332167]
61. Altman JD, Moss PA, Goulder PJ, Barouch DH, McHeyzer-Williams MG, Bell JI, McMichael AJ, Davis MM, Phenotypic analysis of antigen-specific T lymphocytes. Science 274, 94–96 (1996). [PubMed: 8810254]
62. Menk AV, Scharping NE, Moreci RS, Zeng X, Guy C, Salvatore S, Bae H, Xie J, Young HA, Wendell SG, Delgoffe GM, Early TCR Signaling Induces Rapid Aerobic Glycolysis Enabling Distinct Acute T Cell Effector Functions. Cell Rep 22, 1509–1521 (2018). [PubMed: 29425506]
63. Patro R, Duggal G, Love MI, Irizarry RA, Kingsford C, Salmon provides fast and bias-aware quantification of transcript expression. Nat Methods 14, 417–419 (2017). [PubMed: 28263959]
64. Love MI, Huber W, Anders S, Moderated estimation of fold change and dispersion for RNA-seq data with DESeq2. Genome Biol 15, 550 (2014). [PubMed: 25516281]
65. Ignatiadis N, Klaus B, Zaugg JB, Huber W, Data-driven hypothesis weighting increases detection power in genome-scale multiple testing. Nat Methods 13, 577–580 (2016). [PubMed: 27240256]
66. Korotkevich G, Sukhov V, Budin N, Shpak B, Artyomov M, Sergushichev A, Fast gene set enrichment analysis. Biorxiv, (2021). doi: 10.1101/060012
67. Venable JH, Coggeshall R, A Simplified Lead Citrate Stain for Use in Electron Microscopy. J Cell Biol 25, 407–408 (1965). [PubMed: 14287192]

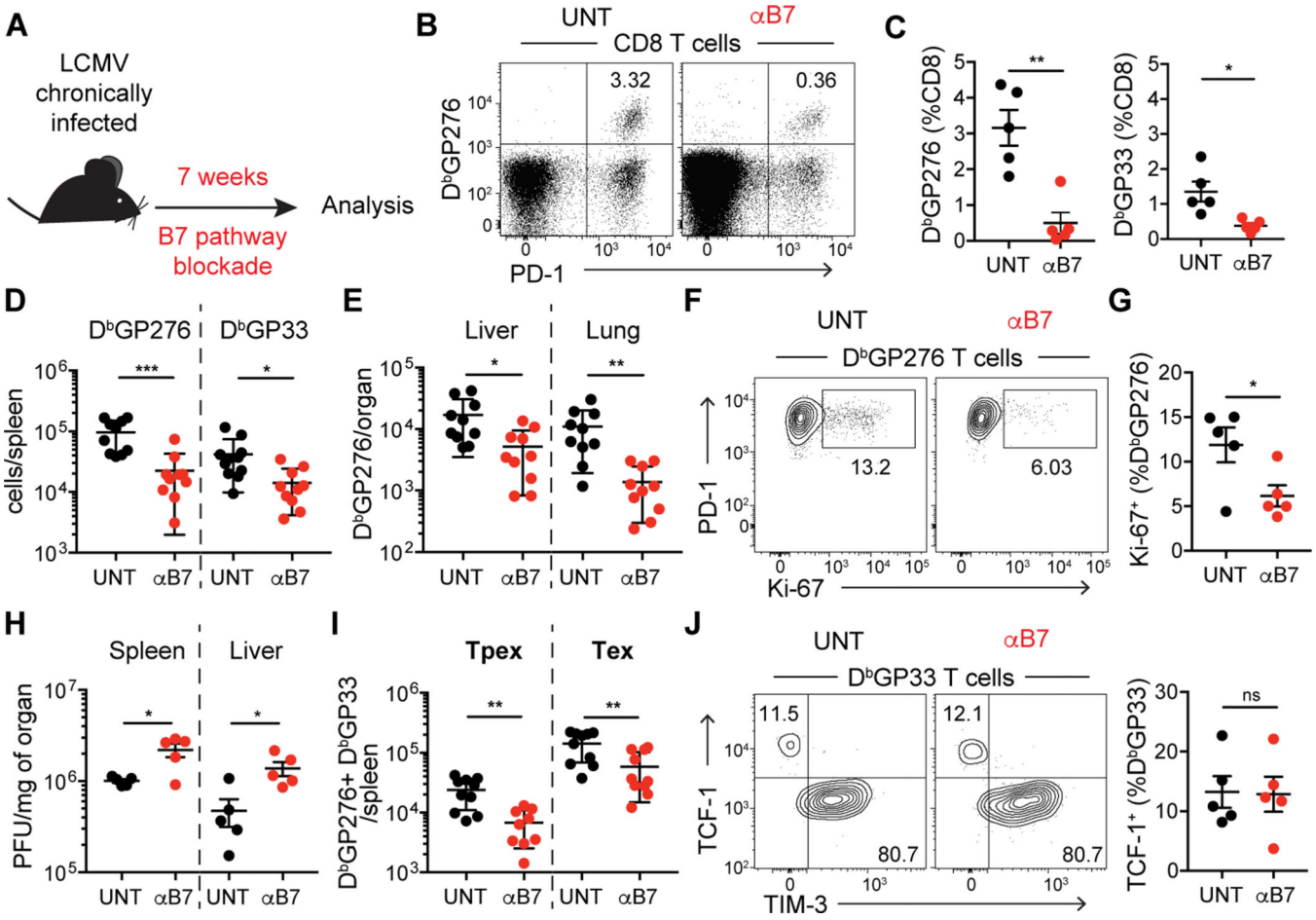

Fig. 1: B7 costimulation is required for the maintenance of virus-specific CD8 T cells during chronic LCMV infection.

(**A**) Experimental layout: C57BL/6J mice were transiently depleted of CD4 T cells and infected with LCMV clone 13. Mice with established life-long chronic infection (>40 days post infection) remained untreated (UNT) or received anti-B7–1 and anti-B7–2 blocking antibodies (αB7) during 7 weeks (wks). (**B** and **C**) Frequency of LCMV-specific CD8 T cells in spleen. (**D** and **E**) Number of LCMV-specific CD8 T cells in different organs. (**F** and **G**) Ki-67 expression on LCMV-specific CD8 T cells in the spleen. (**H**) Viral titer in organs, as quantified by plaque assay. PFU, plaque-forming units. (**I**) Number of splenic LCMV-specific Tpex and Tex. (**J**) Frequency of Tpex (TCF-1$^+$) and Tex (TIM-3$^+$) virus–specific CD8 T cells in spleen. Data in (B, C, F, G, H and J) are representative of 3 independent experiments with 4–5 mice/group. Data in (D, E, and I) show combined data from two of three independent experiments. Symbols represent individual mice, bars show mean value of all animals analyzed and error bars indicate SEM. Significance was determined using unpaired Student's *t-test* *P < 0.05, **P < 0.01, ***P < 0.001. ns, not significant.

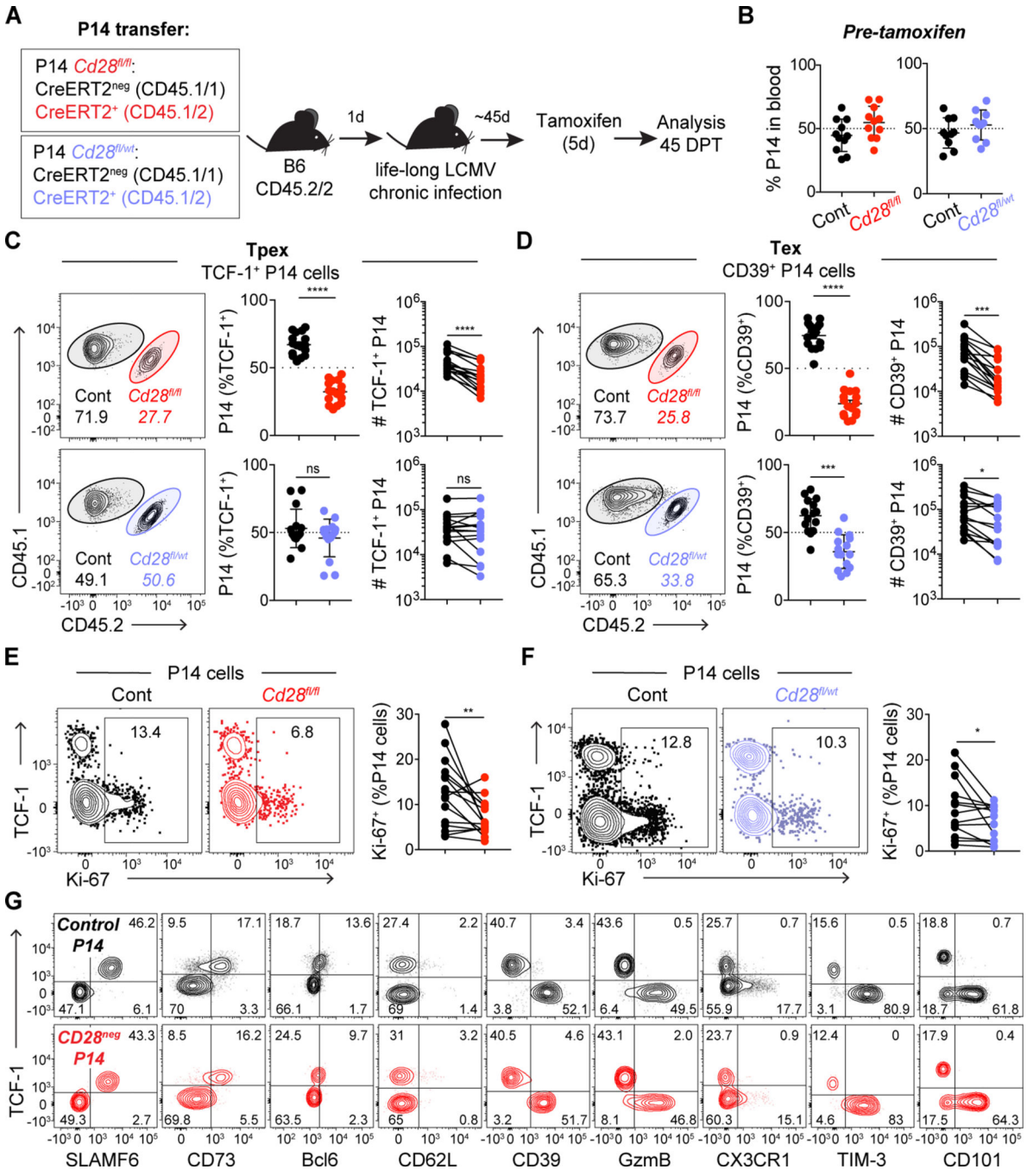

Fig. 2: Level of CD28 expression differentially impacts Tpex and Tex.

(**A**) Experimental layout: *Cd28*$^{fl/fl}$ CreERT2^{neg} (control, black), *Cd28*$^{fl/wt}$ CreERT2^{+} (heterozygous, blue) and *Cd28*$^{fl/fl}$ CreERT2^{+} (homozygous, red) P14 T cells were co-transferred 50:50 (1,000 cells each) to C57BL/6J mice (depleted of CD4 T cells) the day before LCMV clone 13 infection. Mice that had been adoptively transferred with P14 T cells received tamoxifen 45 days post infection (DPI) and analyses in **C-F** were performed in spleen 45 days post tamoxifen (DPT). Analyses in C-F are on the entire population of transferred P14 T cells, without prior gating according to CD28 level. **(B)** Frequency of

co-transferred P14 cells, 45 days post infection (DPI). **(C)** Frequency and absolute number of each P14 T cell population among Tpex (TCF-1^{+}) and **(D)** Tex (CD39^{+}). **(E-F)** Ki-67 expression. **(G)** Representative flow cytometry plots showing phenotypic characterization of P14 T cells: control (black) and *Cd28$^{fl/fl}$* CreERT2^{+} gated on CD28^{neg} (red) as shown in Fig S6A. Data in (B-G) are representative of 3 independent experiments with four to six mice per group. Data in (B) show combined data from two of three independent experiments; (C-F) show combined data of all three independent experiments. Symbols represent individual mice, bars show mean value of all animals analyzed and error bars indicate SEM. Connecting lines between symbols link cells analyzed from the same mouse. Significance in (C-F) was determined using a paired Student's *t-test*. *P < 0.05, **P < 0.01, ***P < 0.001, ****P < 0.0001.

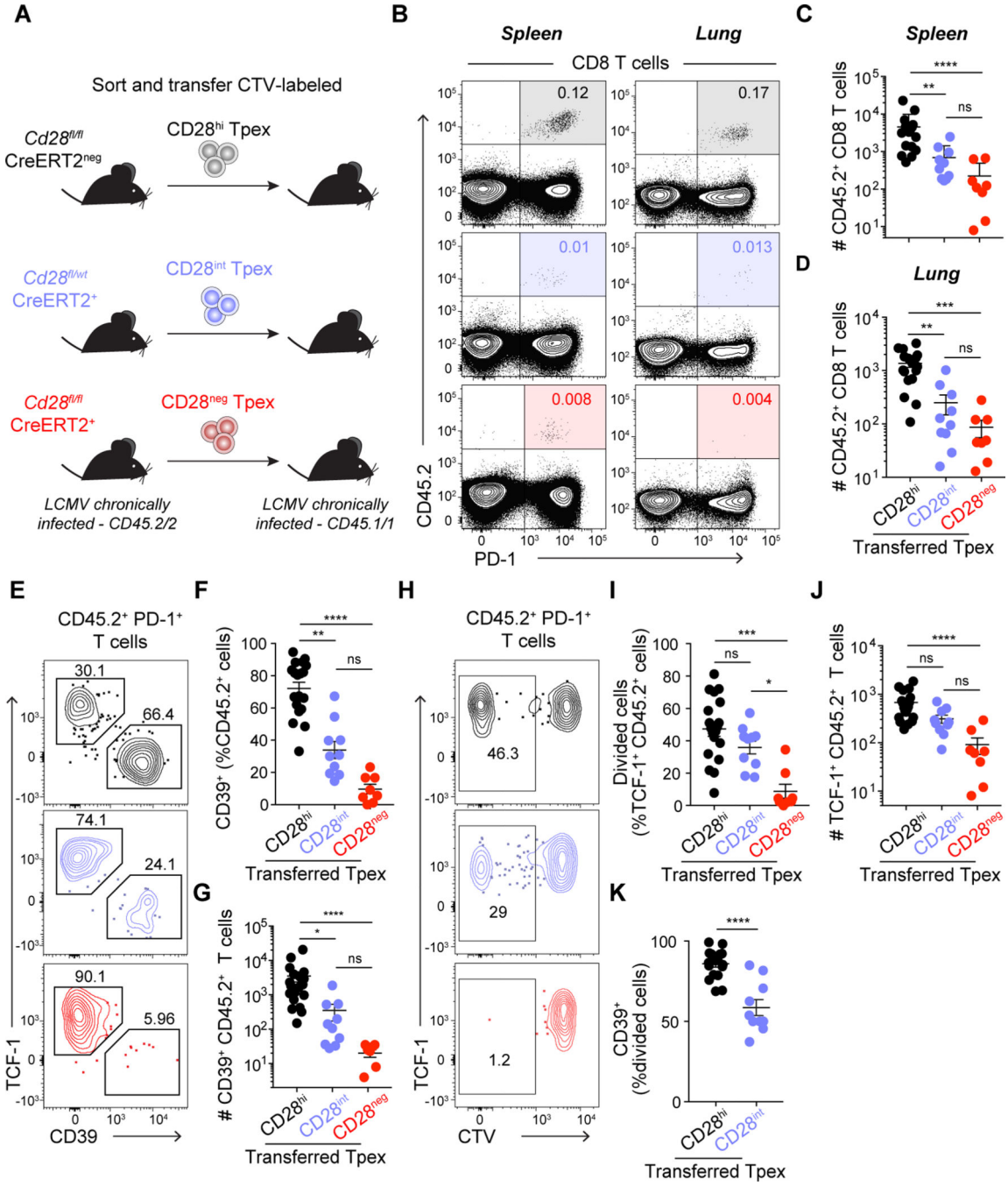

Fig. 3: Level of CD28 expression impacts Tpex self-renewal and differentiation.

(A) Experimental layout: control *Cd28*$^{fl/fl}$ CreERT2^{neg}, heterozygous *Cd28*$^{fl/wt}$ CreERT2^{+} and homozygous *Cd28*$^{fl/fl}$ CreERT2^{+} mice with established life-long LCMV chronic infection received tamoxifen treatment. 15–21 days post tamoxifen, CD28^{hi} (black), CD28^{int} (blue) and CD28^{neg} (red) CD45.2 Tpex were sorted, CellTrace Violet (CTV)-labeled and transferred into infection matched CD45.1 recipients. Analysis was performed 4–5 weeks post-transfer. **(B)** Representative flow cytometry plots showing the frequency of CD45.2^{+} donor cells among CD8 T cells in spleen (left) and lung (right) of CD45.1 recipient

mice. (**C**) Total number of CD45.2$^+$ donor CD8 T cells recovered in spleen and **(D)** lung. **(E)** Representative CD39 and TCF-1 expression on donor CD45.2$^+$ cells in spleen. **(F)** Frequency and **(G)** total number of differentiated donor CD39$^+$ Tex in spleen. (**H-I**) Frequency of divided cells (CTV^{low}) among TCF-1$^+$ CD45.2$^+$ T cells in spleen. **(J)** Total number of donor TCF-1$^+$ Tpex in spleen. **(K)** Frequency of CD39$^+$ differentiated cells among divided (CTV^{low}) transferred cells in spleen. Data in (B-K) are representative of 4 independent experiments with two to five mice per group. Data in (C-D, F-G and I-K) show combined data from all experiments. Symbols represent individual mice, bars show mean value of all animals analyzed and error bars indicate SEM. Significance was determined using (C-D, F-G and I-J) Kruskall-Wallis with Dunn's correction for multiple comparisons, (K) Mann-Whitney. *P < 0.05, **P < 0.01, ***P < 0.001, ****P < 0.0001.

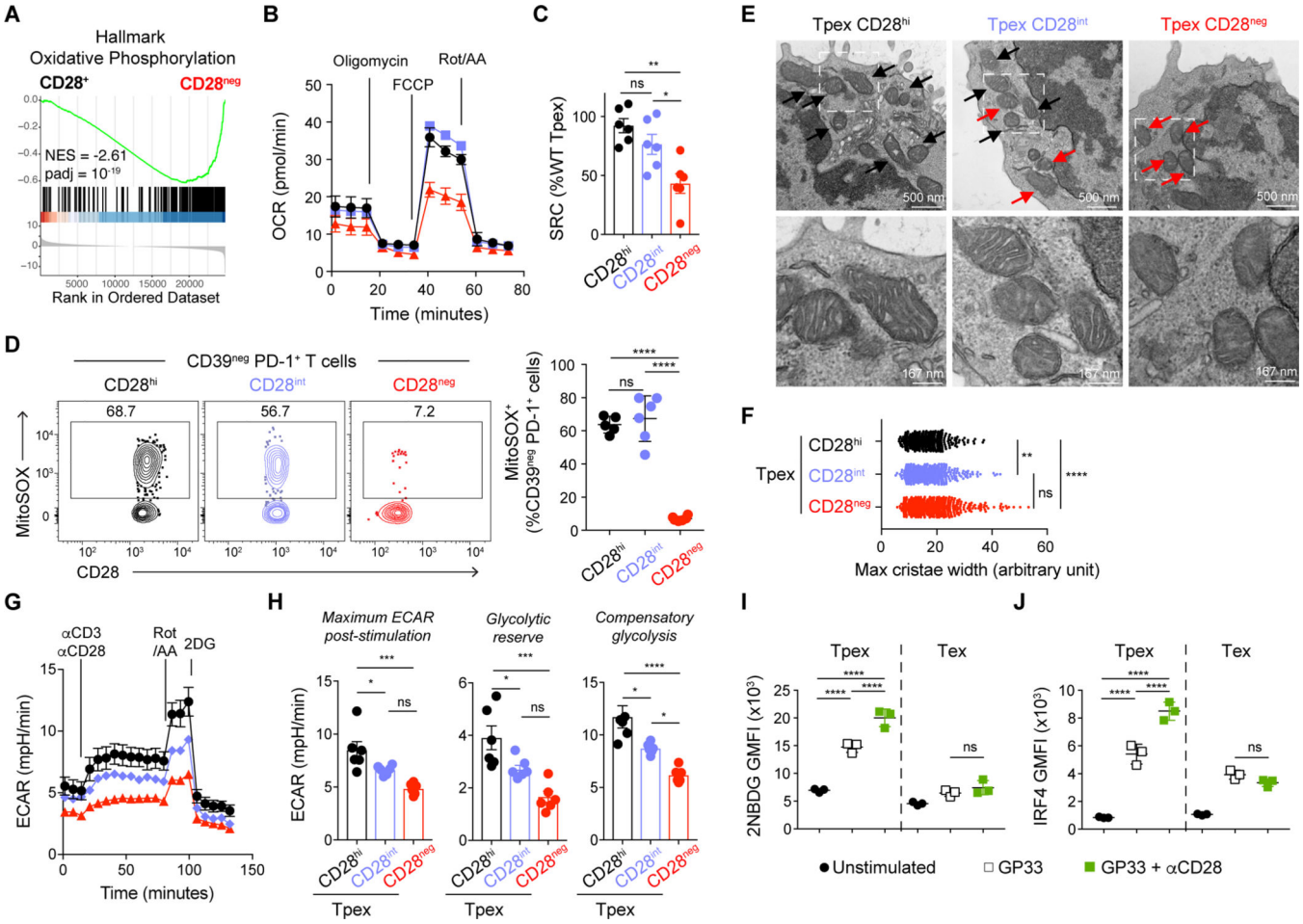

Fig. 4: CD28 regulates Tpex metabolism.

(A) P14 Tpex (CD73^{+} CD39^{neg}) and P14 Tex (CD39^{+}) control (*Cd28$^{fl/fl}$* CreERT2^{neg}) or CD28^{neg} (homozygous *Cd28$^{fl/fl}$* CreERT2) were sorted from life-long LCMV chronically infected mice 2-weeks post tamoxifen for RNA sequencing analysis. Gene set enrichment analysis (GSEA) shows Hallmark Oxidative Phosphorylation gene set in CD28^{+} versus CD28^{neg} Tpex. **(B-H)** Tpex control, CD28^{int} and CD28^{neg} were sorted as described in Fig. 3A and S7A and used for metabolic analysis by seahorse (B, C, G and H) or electron microscopy (E and F). **(B)** Extracellular flux analysis showing oxygen consumption rate (OCR) of sorted CD28^{hi} (control), CD28^{int} and CD28^{neg} Tpex 15 days post tamoxifen. **(C)** Spare respiratory capacity (SRC) calculated as difference between maximal and basal OCR normalized to the mean of control CD28^{hi} Tpex. **(D)** MitoSOX (mitochondrial reactive oxygen species) staining in CD28^{hi} (black, from *Cd28$^{fl/fl}$* CreERT2^{neg} mice), CD28^{int} (blue, from *Cd28$^{fl/wt}$* CreERT2^{+} mice) and CD28^{neg} (red, from *Cd28$^{fl/fl}$* CreERT2^{+}) splenic Tpex from life-long LCMV chronically infected animals, 15 days post tamoxifen. **(E)** Electron microscopy of CD28^{hi}, CD28^{int} and CD28^{neg} sorted Tpex 15 days post tamoxifen. Black arrows highlight healthy mitochondria with organized cristae, red arrows point to disorganized mitochondria. Manification 50000X, scale bar is 500 nm, bottom images are an enlargement (x3) of the field highlighted on top images, scale bar is 167 nm. **(F)** Maximal cristae width, symbols represent measurements for individual crista. (**G**) Extracellular

acidification rate (ECAR) of sorted CD28^{hi} (black), CD28^{int} (blue) and CD28^{neg} (red) Tpex 15 days post tamoxifen. **(H)** Maximum ECAR post-stimulation, glycolytic reserve and compensatory glycolysis of CD28^{hi} (black), CD28^{int} (blue) and CD28^{neg} (red) Tpex. (**I**-**J**) Splenocytes from life-long LCMV chronically infected P14-chimera mice were stimulated with GP33 peptide with or without αCD28. **(I)** 2-NBDG uptake by P14 after 6h of stimulation. (**J**) IRF4 expression on P14 stimulated for 24h. Data in (B and G) are representative of 3 independent experiments with two to three samples per group, symbol represent mean value of all replicates analyzed and error bars indicate SEM. Data in (D, I, and J) are representative of 3 independent experiments with three to five mice per group. Data in (C and H) show combined data from three independent experiments. Symbols show individual replicates (C, H, I and J) or mice (D), bars show mean value of all samples analyzed and error bars indicate SEM. (C, D, F, H, I, and J) Significance was determined using ANOVA with Sidak's correction for multiple comparisons *P < 0.05, **P < 0.01, ***P < 0.001, ****P < 0.0001.

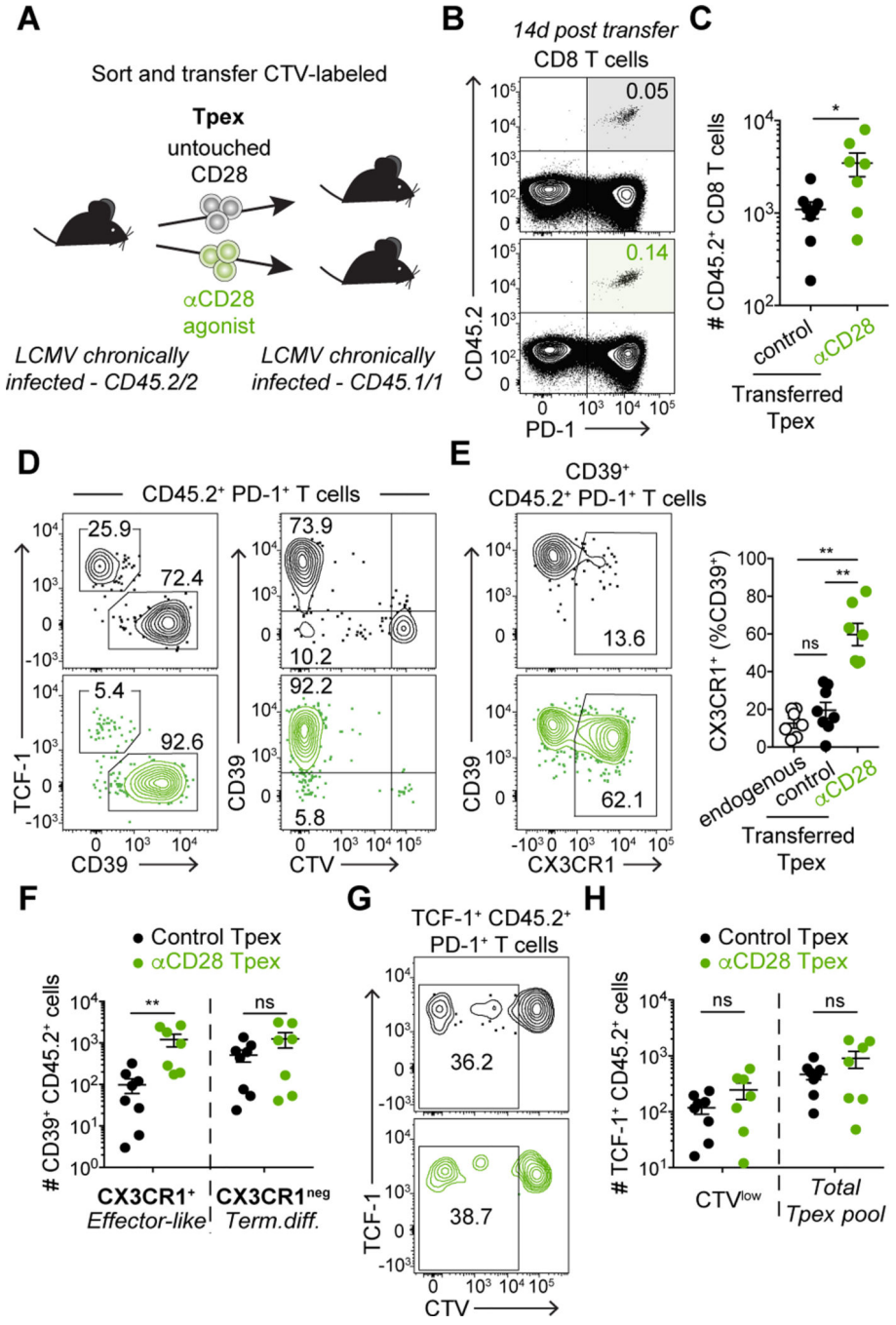

Fig. 5: Enhancing CD28 signaling improves *effector-like* Tex differentiation.

(**A**) Experimental layout: CellTrace Violet (CTV)-labeled CD45.2 $CD39^{neg}$ $PD\text{-}1^{+}$ Tpex sorted from life-long LCMV chronically infected animals were transferred into infection-matched CD45.1 recipient mice. Tpex were sorted without CD28 staining (control, untouched CD28) or with anti-CD28 antibody. (B-H) show data in spleen of recipient mice 14 days post-transfer. (**B**) Frequency and **(C)** Number of $CD45.2^{+}$ donor cells. **(D)** Expression of TCF-1, CD39 and CTV among $CD45.2^{+}$ donor CD8 T cells. (**E**) Frequency of CX_3CR1^{+} effector-like Tex among $CD39^{+}$ Tex cells; endogenous $PD\text{-}1^{+}$ Tex (open circles),

CD28-untouched donor cells (black) and CD28-stimulated donor cells (green). (**F**) Number of *effector-like* Tex ($CX3CR1^+$ $CD39^+$) and terminally differentiated Tex ($CX3CR1^{neg}$ $CD39^+$) $CD45.2^+$ CD8 T cells. **(G)** Representative frequency of divided (CTV^{low}) cells among TCF-1^+ $CD45.2^+$ CD8 T cells. **(H)** Number of divided (CTV^{low}) and total $CD45.2^+$ Tpex. Data in (B-H) are representative of 2 independent experiments with three to five mice per group. Data in (C, E, F and H) show combined data from two independent experiments. Symbols represent individual mice, bars show mean value of all animals analyzed and error bars indicate SEM. Significance was determined using (C, F and H) Mann-Whitney, (E) Kruskall-Wallis with Dunn's correction for multiple comparisons *P < 0.05, **P < 0.01.